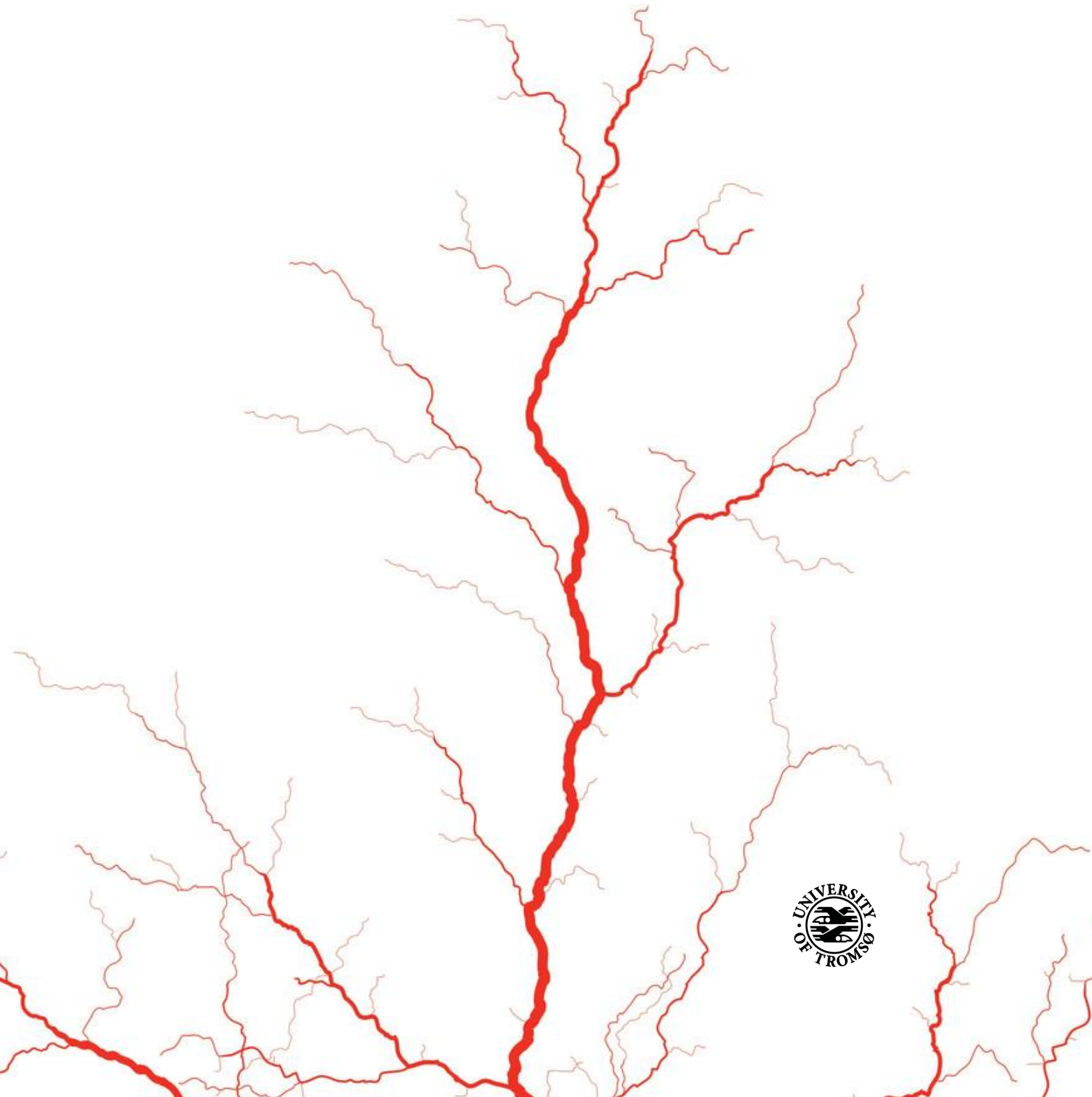


# Brain capillarization in diving mammals: a selection of staining and quantification methods

—  
**Chiara Ciccone**

*BIO-3950 Master thesis in Biology*  
*May 2019*





# Brain capillarization in diving mammals: a selection of staining and quantification methods

—  
**Chiara Ciccone**

*BIO-3950 Master thesis in Biology*

*May 2019*

## **Supervisor**

Lars P. Folkow, University of Tromsø – The Arctic University of Norway – UiT

## **Co-supervisor**

Samuel J. Geiseler, University of Oslo – UiO



UiO : **University of Oslo**



Cover picture taken from <https://www.vectorstock.com/>

*A mia madre. Di nuovo.*

And God said: “Let the waters be full of living things, and let birds be in flight over the earth under the arch of heaven”. And God made great sea-beasts, and every sort of living and moving thing with which the waters were full, and every sort of winged bird: and God saw that it was good. And God gave them His blessing, saying: “Be fertile and have increase, making all the waters of the seas full, and let the birds be increased in the earth”.  
And there was evening and there was morning: the fifth day.

*Genesis 1, 20-23*

«Se nu te scierri mai de le radici ca tieni,  
Rispetti puru quiddre de li paisi luntani.  
Se nun te scierri mai de du ete ca sta ieni,  
Dai chiù valore alla cultura ca tieni»<sup>1</sup>

*Le radici ca tieni, Sud Sound System*

---

<sup>1</sup> “If you never forget about the roots that you have,  
You’ll respect also the ones of distant countries.  
If you never forget about where you come from,  
You’ll give more value to the culture that you have”.



## Acknowledgements

First of all, I would like to thank my two supervisors, Lars Folkow and Samuel Geiseler: thank you for giving me this project, for your trust and for believing in my capability and reassuring me when panic was taking over. Having the chance of working with you has been one of the principal reasons that brought me to Tromsø, and I am honoured that I can say that it was you who guided me in my first steps as a «true scientist».

I also would like to thank Cecilie Morland and her «Brain group» at the University of Oslo: thank you for hosting me (even if just for two weeks) and for all the help with my lab work. Thanks also to Hallvard Lauritz Olsvik for the technical support with the confocal microscope and to the Department of Medical Biology for giving me the chance to use their instruments.

A huge thanks goes to my office mates for tolerating me and my “concerts”. A special thank goes to Sandra: thank you for your craziness, for all our ridiculous nights out and, most of all, for your friendship.

Gabrielle, even if you just moved to Tromsø, you helped me a lot. I am really looking forward to having the chance to share an office with you.

Thanks to all those who, even if far, managed to stay close to me.

Vero and Simo: thank you for listening me, for giving me the strength to face the most difficult moments and for never doubting me. You are the sisters that I never had.

Chiara, thank you for these 22 years and remember: «When the snow falls and the cold winds blow, the lone wolf perishes, but the pack survives».

«IL Paolo» also deserves to be thanked: if you weren't so crazy to move here, I probably would have never arrived here either. Thank you for your patience and for giving me all the help that I needed.

Thanks to all Casa Inferno staff. Thank you for giving me a job, for literally giving me a place where to live, but mostly thank you for making me feel like at home. You have been and will always be the closest thing to a family that I have here, and I will never thank you enough for this.

The biggest thank goes to my family. Thank you for not thinking that I was a fool when I decided to move to Norway, thank you for understanding me and for not trying to stop me.

Sara and Luca, you have been crucial. Without your support I could have never make it.

Mum, thank you for letting me go, for being a «great woman» and for scarifying so much only for me. Thank you for being the best mother and father that a daughter could ask for.





## Abstract

Diving species can cope with acute and repeated hypoxia through adaptations that are absent in non-diving animals. One of the greatest challenges to deal with during diving is the lowering of the arterial oxygen pressure ( $P_aO_2$ ), which causes a decrease in the driving force for the oxygen diffusion from the capillaries to the cells. My hypothesis is that the marine mammalian brain shows improved brain blood flow through a denser capillarization which shortens the distance between the capillaries and the cells, allowing the lower  $PO_2$  gradient to achieve a sufficient rate of  $O_2$  supply to the neural tissue. To study this, a reliable method for determining the capillary density needs to be found. The principal aim of this project is to validate a method to stain and visualize the capillaries and to use this as an initial test to verify the hypothesis that the seal brain shows higher capillarization, when compared to terrestrial mammals as a general adaptation to hypoxia. Several studies have shown that there is a relation between the metabolic activity and the degree of capillarization of a certain tissue. This hypothesis, that brain regions with different metabolic demands (i.e. grey and white matter) can show dissimilar levels of capillarization, is here tested as well. The brains of 2 harp seals (*Pagophilus groenlandicus*), 1 hooded seal (*Cystophora cristata*) and 2 reindeer (*Rangifer tarandus*) were collected. Samples were taken from the frontal and visual cortex, the hippocampus, the cerebellum and the medulla, since these regions were previously reported to have different capillary densities. After a detailed analysis of different staining techniques, capillaries were identified by immunostaining the collagen IV of their basement membrane and visualized at the confocal microscope. The images obtained were then subjected to two different quantification methods and results were compared. The method that is indicated as “automatized method” turned out to be more reliable and also easier to apply to the images. Since the anti-collagen IV technique gave a good quality stain in both the species studied here, it is concluded that its use and the following application of the “automatized method” as a quantification method is a reliable combination for assessing the degree of capillarization of cerebral tissue. In general, both the hypothesis that diving species have an enhanced brain capillarization and that regional differences occur between cerebral regions are confirmed but further investigations with a higher number of samples are needed to better assess this hypothesis.

## List of abbreviations

ANLS	Astrocyte-neuron lactate shuttle
CB	Cerebellum
CNS	Central nervous system
Coll-IV	Collagen type IV
DG	Dentate gyrus
FC	Frontal cortex
fO <sub>2</sub>	Oxygen flux through a capillary
FO <sub>2</sub>	Total oxygen flux
HC	Hippocampus
HIF-I	Hypoxia-inducible factor I
LDH	Lactate dehydrogenase
MED	Medulla
MTT	Mean transit time
O <sub>2</sub>	Oxygen
P <sub>a</sub> O <sub>2</sub>	Arterial oxygen pressure
PO <sub>2</sub>	Oxygen pressure
SGZ	Subgranular zone
SVZ	Subventricular zone
UEA-I	<i>Ulex europaeus</i> agglutinin-I
VC	Visual cortex
VEGF	Vascular endothelial growth factor
vWF	Von Willebrand factor

## ***Table of contents***

<b><i>Abstract</i></b> .....	<b>7</b>
<b><i>List of abbreviations</i></b> .....	<b>8</b>
<b>1. <i>Introduction</i></b> .....	<b>11</b>
1.1 Marine mammals .....	11
1.2 Adaptations to diving.....	11
1.3 Brain energetics .....	13
1.3.1 Normoxic conditions.....	13
1.3.2 Hypoxic conditions .....	14
1.3.3 Intrinsic hypoxia tolerance.....	15
1.4 Tissue capillarization.....	16
1.4.1 Capillaries identification.....	18
1.5 Studies on marine mammals .....	19
1.6 Aims of the study.....	20
1.7 Hooded seal .....	21
1.8 Harp seal .....	22
1.9 Reindeer .....	23
<b>2. <i>Materials and methods</i></b> .....	<b>24</b>
2.1 Animals.....	24
2.2 Tissue sampling .....	26
2.3 Sectioning .....	27
2.4 Immunostaining .....	29
2.5 Confocal microscopy.....	30
2.6 Quantitative analysis.....	32
2.6.1 Counting crosses method.....	33
2.6.2 Automated method .....	34
2.7 Statistic .....	36
<b>3. <i>Results</i></b> .....	<b>37</b>
3.1 Differences between methods.....	37
3.2 Counting crosses method.....	38
3.3 Automated method.....	39
<b>4. <i>Discussion</i></b> .....	<b>41</b>
4.1 Staining technique selection .....	41
4.2 Methodological considerations .....	44
4.3 Differences between species .....	45
4.4 Regional differences .....	48
4.4.1 Cerebral and cerebellar cortex .....	48
4.4.2 Medulla.....	53
4.4.3 Hippocampal subregions.....	53
<b>5. <i>Conclusions</i></b> .....	<b>57</b>

<b>6. <i>References</i> .....</b>	<b>58</b>
<b>7. <i>Appendixes</i> .....</b>	<b>66</b>

# 1. Introduction

## 1.1 Marine mammals

Marine mammals are generally divided into two main systematic orders: pinnipeds (*Pinnipedia*), which include seals and walruses, and cetaceans (*Cetacea*), which is constituted by whales and dolphins. Cetaceans are usually differentiated into *Odontoceti* and *Mysticeti*, commonly known also as toothed and baleen whales. Pinnipeds are instead divided into three groups: *Phocidae*, also named “true seals”, *Otariidae*, or “eared seals”, and *Odobenidae*, which is constituted only by the walrus.

Despite the subdivision in several groups, all these animals have to face the same challenge, that is a life underwater. This condition exposed these organisms to an evolutionary selection pressure that led to the development of several adaptations, both behavioural and physiological, which made them able to survive in an environment as challenging as the marine one (reviews: Butler and Jones, 1997; Ramirez et al., 2007).

## 1.2 Adaptations to diving

In order to avoid drowning, diving species need to stop breathing when they start to dive. But, since all the tissues and their cells will still be metabolically active, the arterial oxygen ( $O_2$ ) content will start decreasing, while the arterial carbon dioxide ( $CO_2$ ) content will increase (Scholander, 1940).

Diving mammals, like pinnipeds, can cope with the decline of the blood  $O_2$  content because of their enhanced capacity for tissue  $O_2$  storage in both blood and muscles which makes them able to rely on the aerobic metabolism also during diving (Scholander, 1940; Burns et al., 2007). Crucial for this are the large blood volume, with an elevated hemoglobin concentration and haematocrit, which indicates the percentage of the blood volume occupied by erythrocytes, and the large muscle mass with a high myoglobin concentration (Burns et al., 2007; Lestyk et al., 2009).

In pinnipeds, the haematocrit can exceed 60% while the blood hemoglobin concentration can reach levels up to 25 g/100 ml (Lenfant et al., 1970; Qvist et al., 1986). In a study by Burns et al. (2007) on the hooded (*Cystophora cristata*) and the harp seal (*Pagophilus groenlandicus*), it was shown that these species can have a blood volume of 194 ml/kg and 169 ml/kg, respectively, while in man the average blood volume is around 75 ml/kg (Gregersen and Rawson, 1959). The high blood volume also implies a very high body O<sub>2</sub> store, that was found to be 89.5 ml/kg for the hooded seal and 71.6 ml/kg for the harp seal (Burns et al., 2007). Even though there is a difference between deep and shallow-divers, they both show higher myoglobin concentration compared to terrestrial animals, the highest level recorded being 94 mg/g ca. in the hooded seal (Burns et al., 2007), which is quite impressive compared to the 29.25 mg/g found in the human skeletal muscle (Nemeth and Lowry, 1984).

Although the O<sub>2</sub> stored in the body is greater in diving mammals than in non-diving ones, it is insufficient to enable them to maintain an aerobic metabolism and stay submerged for periods as long as 1 or 2 hours (Scholander, 1940; Butler and Jones, 1997). The O<sub>2</sub> stores must be conserved for those tissues that are highly hypoxia sensitive and have a low anaerobic capability, such as the heart and the brain (Dormer et al., 1977; Zapol et al., 1979; Blix et al., 1983)

Diving animals respond to prolonged submergence with a reduction of the heart rate, called bradycardia (Scholander, 1940), together with a selective peripheral arterial constriction which ensures that the reduced cardiac output is preferentially redistributed to the heart and the brain (Zapol et al., 1979; Blix et al., 1983).

In a study by Blix et al. (1983) on the spotted seal (*Phoca vitulina larga*) and the grey seal (*Halichoerus grypus*), it was shown that almost all the visceral organs displayed a marked reduction of blood flow during dives to or approaching zero flow. Even though at the beginning of the dive the brain blood flow showed a ~50% reduction, as soon as the maximum dive capacity was approached, it reached levels that were well above the pre-dive ones (Blix et al., 1983). These results were in accordance also with other studies conducted on different phocid species (Kerem and Elsner, 1973; Dormer et al., 1977; Zapol et al., 1979). The redistribution of the blood flow was always combined to an almost 90% reduction of the cardiac output (Blix et al., 1983; Zapol et al., 1979) and heart rates as low as 7 beats/min have been recorded (Murdaugh et al., 1961). However, such extreme responses, that are usually referred to as “diving response”, are more part of a gradual process rather than an “all-or none” response: the

intensity of the bradycardia increases as a function of the dive duration and, during experimental conditions (forced dives), more immediate and extreme responses are recorded compared to free-diving conditions (Blix, 1987; Hill et al., 1987; Thompson and Fedak, 1993).

### 1.3 Brain energetics

The brain is a highly aerobic organ and, although it constitutes only a small fraction of the total body weight, it accounts for a large percentage of the total O<sub>2</sub> consumption: in humans at rest, approximately 20% of the O<sub>2</sub> is consumed by the brain even though it accounts for only 2% of the body weight (Erecinska and Silver, 1989; Erecinska and Silver, 2001). Indeed, the brain is committed to a continual active state and, therefore, it has an obligatory high level of energy consumption (Lutz et al., 2003).

#### 1.3.1 Normoxic conditions

The maintenance of all cerebral functions depends on a continuous supply of ATP and, since the primary mechanism by which ATP is produced is the mitochondrial oxidative phosphorylation, the brain depends also on a constant supply of O<sub>2</sub> to generate ATP at sufficient rates (Erecinska and Silver, 1989; Erecinska and Silver, 2001). Under normoxic conditions more than 95% of brain ATP is produced aerobically through the oxidative phosphorylation: the complete combustion of 1 mole of glucose by 6 moles of O<sub>2</sub> produces 36 moles of ATP (Erecinska and Silver, 1989; Erecinska and Silver, 2001; Lutz et al., 2003).

Around 40-60% of the ATP produced is used for the ion pumping needed to maintain the different distribution of ions on either side of neurons' membranes (Na<sup>+</sup>, K<sup>+</sup>, Cl<sup>-</sup> and Ca<sup>2+</sup>). This generates an electrochemical disequilibrium around the neuronal membrane called "membrane potential" (Erecinska and Silver, 1994; Erecinska and Silver, 2001; Lutz et al., 2003; Larson et al., 2014). The diverse concentrations of ions around the cell membranes are maintained by specialized membrane proteins, known as ion pumps. The ATPase, also called Na<sup>+</sup>/K<sup>+</sup> pump, is the one that consumes the largest proportion of ATP: it transfers 3 Na<sup>+</sup> ions out and 2 K<sup>+</sup> ions into the cell for each molecule of ATP consumed (Lutz et al., 2003; Erecinska and Silver, 2001).

The normal functions of the central nervous system (CNS), like the generation, processing and transmission of impulses, can be accomplished only if this electrochemical disequilibrium is maintained (Erecinska and Silver, 1994).

The pivotal role of O<sub>2</sub> in the production of ATP, makes the brain dependent on an interrupted supply of O<sub>2</sub> which, if limited or disrupted even for a few seconds, can lead to severe neuronal damages, including cell death (Erecinska and Silver, 1989; Lutz et al., 2003; Lipton, 1999).

### 1.3.2 Hypoxic conditions

Due to its high demand of energy, the brain is particularly sensitive to limitation of O<sub>2</sub> supply (Erecinska and Silver, 2001). The state of deficiency in O<sub>2</sub> availability to, or utilization by, body tissues is defined as hypoxia (Ramirez et al., 2007), and it occurs in the CNS when the metabolic demand cannot be met by a matched O<sub>2</sub> delivery (LaManna et al., 2004).

In cases of severe O<sub>2</sub> limitation, excitable cells cannot meet the energy demands of the active ion-transporting systems (Boutilier, 2001). Indeed, as the O<sub>2</sub> flow to tissues decreases, the oxidative phosphorylation is blocked, and the anaerobic glycolysis is the only pathway by which ATP can be generated: per each mole of glucose, 2 moles of ATP are produced (Erecinska and Silver, 1989; Boutilier, 2001; Erecinska and Silver, 2001; Lutz et al., 2003; Larson et al., 2014).

Because of its low efficiency, the anaerobic ATP production cannot sustain the pre-existing energy demands for more than a few minutes or hours: the fall in ATP levels, will lead to energy imbalance and to a decline of all the ATP-dependent neuronal process (Boutilier, 2001; Lutz et al., 2003; Larson et al., 2014). The Na<sup>+</sup>/K<sup>+</sup> pump will not be able to maintain the ions gradient among the cellular membrane and changes in the ions' distribution are rapidly seen (Erecinska and Silver, 2001). Because of the failure of the ion gradients, neurons depolarize, resulting in the activation of multiple internal cascades that lead to cell damages and, if the O<sub>2</sub> is not quickly re-introduced, cells die (Leblond and Krenjević, 1989; Dirangl et al. 1999; Erecinska and Silver, 2001).



### 1.3.3. Intrinsic hypoxia tolerance

By contrast, seals' brain displays a remarkable tolerance to prolonged periods of low O<sub>2</sub> supply (Elsner et al., 1970; Kerem and Elsner, 1973; Qvist et al., 1986). Neurons of isolated slices of hooded seal brain are capable to remain active until  $19 \pm 10$  min of hypoxia exposure, or even up to 60 min (Folkow et al., 2008) and, it has been suggested that such ability is due to intrinsic properties of the neurons, like biochemical adaptations on an enzymatic level. It was believed that the seal brain had a higher capacity of anaerobic metabolism because of the distribution and activity pattern of the enzyme lactate dehydrogenase (LDH) found in this tissue (Blix and From, 1971; Murphy et al., 1980). This enzyme can exist in five different isoforms (LDH1, LDH2, LDH3, LDH4 and LDH5), composed by different combinations of two principal subunits, LDH-A and LDH-B, whose activity is correlated to the anaerobic capacity of the tissue in which they reside (Cahn et al., 1962; Markert, 1963; Dawson et al., 1964). Particularly, LDH-A catalyzes the conversion of pyruvate to lactate, favouring the anaerobic metabolism, while LDH-B converts lactate to pyruvate in favour of the oxidative pathway (Cahn et al., 1962; Dawson et al., 1964). In a recent study (Hoff et al., 2016), an extensive analysis of LDH was performed in brain of hooded seals, ferrets and mice and it was shown that the hooded seal brain does not have an enhanced anaerobic capacity compared to terrestrial species. However, it was found that the hooded seal brain has a higher proportion of LDH1 and LDH2 isoforms, which are mainly composed by LDH-B subunits, suggesting an enhanced capacity for lactate oxidation, that can be very beneficial during the recovery phase to remove all the lactate accumulated while diving (Hoff et al., 2016).

According to the classic astrocyte-neuron lactate shuttle (ANLS) hypothesis, depending on the distribution of the different LDH isoforms, the conversion of pyruvate to lactate occurs in astrocytes, while the conversion of lactate to pyruvate occurs in neurons (Bittar et al., 1996). Hoff et al. (2016) showed that in the hooded seal the opposite seems to happen: astrocytes resulted LDH-B positive, suggesting that in seals brain the conversion of lactate to pyruvate occurs mainly in the astrocytes, while neurons convert pyruvate to lactate. This "reverse" ANLS hypothesis implies that seals' neurons can work mainly anaerobically (Mitz et al., 2009), giving an explanation to their remarkable tolerance to hypoxic conditions (Folkow et al., 2008; Geiseler et al., 2016).

Apart from these intrinsic properties of the neurons, other adaptations more on a tissue rather than cellular level can also occur, like a denser capillarization.

## 1.4 Tissue capillarization

As described by Krogh (1922), the circulatory system is composed by a small number of subordinate systems with quite distinct functions. The heart is the propulsive organ from which the system of arteries (the distributing organ) has to transport the blood to the tissues; at the tissue level, the capillaries are the site at which the exchange of substances between the blood and cells occur; finally, the system of veins (the collecting organ) carries the blood back to the heart (Krogh,1922).

The exchanging of substances is one of the most important function of the circulatory system and the degree at which it occurs depends on the permeability of the capillary wall, which varies from organ to organ (Crone, 1963) (Figure 1). The variations in permeability are related to the morphological modifications of the capillary walls and their endothelial cells in the different organs (Bennett et al., 1959).

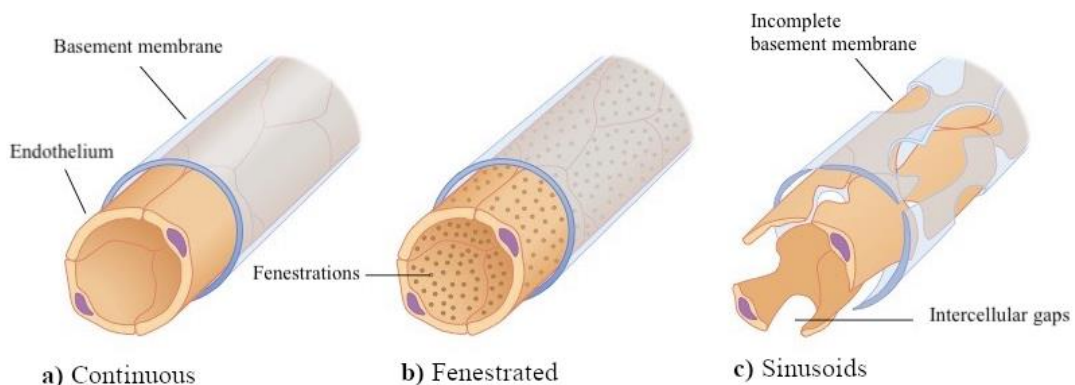


**Figure 1.** Illustration of the different types of capillaries. **a)** Continuous capillary: the endothelium is surrounded by a continuous extracellular matrix called basement membrane. **b)** Fenestrated capillaries: the basement membrane is complete, but the endothelium presents fenestrations or pores. **c)** Sinusoids: the basement membrane is not continuous, and the endothelial cells are separated by intercellular gaps.

Image taken from <https://ib.bioninja.com.au/welcome-to-the-bioninja/> and modified in GIMP-2.10

O<sub>2</sub> is soluble in water and in fluids like the blood and, in its dissolved state, it can spread by the mechanism of diffusion from any point where its concentration is higher to all the other points where its concentration is lower (Krogh, 1922). Therefore, the rate of O<sub>2</sub> diffusion depends

upon its concentration gradient (Krogh, 1922), which is represented by the difference in oxygen pressure ( $PO_2$ ) between capillaries ( $PO_{2c}$ ) and the surrounding tissues ( $PO_{2t}$ ).

According to Krogh's theory (1918; 1922), the  $O_2$  flux ( $fO_2$ ) through a capillary of radius  $r$  to a cylindrical surrounding tissue of radius  $R$  is inversely related to the diffusion distance ( $R - r$ ) and proportional to the  $PO_2$  gradient ( $PO_{2c} - PO_{2t}$ ) (Granger and Shepherd, 1973):

$$fO_2 = K_1 \frac{(PO_{2c} - PO_{2t})}{(R - r)}$$

Where  $K_1$  is a constant. Taking into account the total number of capillaries present in a tissue (capillary density =  $N$ ), the total  $O_2$  flux ( $FO_2$ ) in a tissue can be expressed as follow (Granger and Shepherd, 1973):

$$FO_2 = N fO_2$$

Therefore,  $FO_2$  is directly proportional to the density of capillaries in a tissue ( $N$ ) and inversely proportional to the diffusion distance ( $R - r$ ).

The oxygen concentration of the capillary blood and its  $PO_{2c}$  are functions of the arterial oxygen concentration, which is in turn related to the arterial oxygen pressure ( $P_aO_2$ ) (Granger and Shepherd, 1973). Since  $PO_{2t}$  is almost zero,  $P_aO_2$  represents the main driving force for the diffusion across the capillary wall and any decrease of such value causes a decrease in the delivery of  $O_2$  to the tissues (Granger and Shepherd, 1973; LaManna et al., 2004; Xu and LaManna, 2006). The critical  $P_aO_2$  for the adult non-diving mammalian brain, i.e. the tension at which impairments from limitation in ATP production are first seen, is 25-40 mmHg and, as already stated, values lower than these can cause serious damages (Erecinska and Silver, 2001; Lutz et al., 2003).

It has been shown that, during a long-duration dive, a seal can experience very low  $P_aO_2$  (Scholander, 1940): values lower than 20 mmHg have been recorded (Qvist et al., 1986; Meir et al., 2009). It is likely that, in diving mammals, the decrease in the  $P_aO_2$  and, thus, in the main driving force for the diffusion, can be compensated by an enhanced capillarization of the tissues, which results in a shorter diffusion distance and an improved  $FO_2$  (Granger and Shepherd, 1973; Boero et al., 1999; LaManna et al., 2004).

Evidences of enhanced capillarization have already been presented as an effect of training in human skeletal muscle and in flight-muscles of birds adapted to high altitude (Hather et al., 1991; León-Velarde et al., 1993; Mathieu-Costello et al., 1998; Cocks et al., 2013). In a study by Jensen et al. (2004) it was shown that, in human skeletal muscle, the increased capillarization induced by an intermittent endurance training was combined with an increase in endothelial cells proliferation.

Indeed, several studies suggested that prolonged exposure to hypoxia and the consequent activation of the anaerobic metabolism could trigger angiogenesis in rat and mice brains, resulting in a decreased O<sub>2</sub> diffusion distance (La Manna et al., 1992; Patt et al., 1997; Morland et al., 2017). It has been observed that, in tissue culture, some of the genes involved in the process of angiogenesis are independently responsive to hypoxia (Otrock et al., 2007). Particularly, the hypoxia-inducible factor-I (HIF-I) is most likely the element initiating the process: it upregulates the transcription of the vascular endothelial growth factor (VEGF), which in turn stimulates the proliferation of endothelial cells and, therefore, the formation of new blood vessels in hypoxic tissues (Forsythe et al., 1996; Otrock et al., 2007).

The denser capillarization is an adaptation that allows higher O<sub>2</sub> diffusion conductance, especially in a situation of hypoxemia, so that even lower PO<sub>2</sub> gradients can achieve an adequate rate of O<sub>2</sub> supply (Boero et al., 1999).

#### 1.4.1 Capillaries identification

Many attempts to stain capillaries have been done in the past years by the use of several techniques, especially in the skeletal muscle (Čebašek et al., 2004). Different staining techniques can have different advantages and disadvantages. For example, the toluidine blue staining (Russell et al., 1998; Ludvigsen, 2010) is a histological method whose efficiency depends on the presence of erythrocytes in the vessel lumen (Geyer et al., 1978, only abstract), making the non-perfused vessels poorly recognizable. Enzyme-histochemical methods, like the alkaline-phosphatase staining (Francois-Dainville et al., 1986; LaManna et al., 1992) and the amylase-periodic acid Schiff (PAS) staining (Andersen, 1975), are strictly connected to the enzyme activity whose variations could easily lead to inconsistent results.

In other studies, antibodies against the endothelium (Figure 1) have been used, like the von Willebrand factor (vWF) and lectins (Alroy et al. 1987; Kuzu et al., 1992; Hansen-Smith et al., 1992; Jesmin et al., 2003; Rufaihah et al., 2011). As for the enzyme-histochemical methods,

the results obtained can show great variations. Particularly, the vWF expression on the endothelial cells is not homogenous, but it varies along the vascular tree (Kuzu et al., 1992; Yamamoto et al., 1998; Pusztasteri et al., 2006), while lectins have been proved to have a species-specific binding pattern (Alroy et al., 1987).

Immunohistochemical methods for staining the basement membrane of capillaries have also been employed (Madsen and Holmskov, 1995; Morland et al., 2017). The basement membrane is an external layer that surrounds the endothelium of the capillaries (Bennett et al., 1959) (Figure 1) and whose main component is the collagen type IV (Coll-IV) (Seki et al., 1998). The use of antibodies against Coll-IV of the basement membrane was used for the first time by Madsen and Holmskov (1995) in the human skeletal muscle and it was also employed in more recent studies (Weber et al., 2008; Zhang et al., 2014; Morland et al., 2017) in different cerebral regions of mice and monkeys. In a study by Qu et al. (1997), a nice comparison of different staining techniques for the detection of capillaries was given. Particularly, the use of antibodies against Coll-IV appeared to give reliable results, confirming what was already found by Madsen and Holmskov (1995). Also, since the Coll-IV is the only type of collagen present in the basement membrane (Stephens et al., 1982), the possibility to stain vessels other than capillaries is quite reduced, even though, to some extent, vessels like venules or arterioles can still be stained but they can be easily identified and excluded from the analysis due to the different size. Given this scenario, it is understandable that the choice of an appropriate staining technique for the identification of capillaries is not straightforward, mostly for all the factors that may influence the results (presence of erythrocytes, enzyme activity, species-specificity, etc.).

For this project, the use of antibodies against Coll-IV appeared particularly promising, mostly because of its simplicity and because it showed to give reliable results in different species (humans, monkeys and mice)(Madsen and Holmskov, 1995; Weber et al., 2008; Zhang et al., 2014; Morland et al., 2017).

## 1.5 Studies on marine mammals

A first study about the capillary density in seal's brain was done by Kerem and Elsner (1973) in the cortical grey matter of the Northern elephant seal (*Mirounga angustirostris*). Their results showed that the density of capillaries in the Northern elephant seal's brain are particularly high when compared to the values obtained for man and other mammals in different studies. But both the staining technique and the quantitative method that were used in the study are not well

described in the paper and, knowing what kind of method has been used is fundamental to understand the validity of the data reported.

A few years later, it was demonstrated that the mean density of capillaries was higher in almost all cortical layers of the dolphin (*Stenella coeruleoalba*) than in other terrestrial mammals, like the cat or the rat (Glezer et al., 1987). The highest density of microvessels was found in the layer II of the cerebral cortex and it coincided with the highest neuronal concentration (Glezer et al., 1987). Brain samples were double-stained with uranylacetate and lead citrate, but the use of lead stain can bring to different results depending on the protocol employed (Karnovsky et al., 1961).

An attempt to study brain capillarization in the hooded seal (*Cystophora cristata*) was done by Ludvigsen (2010). The values obtained were quite high when compared to the mouse, the cat and the rat but they were not higher than the ones reported by Kerem and Elsner (1973) for the Northern elephant seal. In this study (Ludvigsen, 2010) capillaries were identified by staining the erythrocytes. Because of this, the risk of underestimate the total number of capillaries is high since the non-perfused ones will not be recognized. Also, since the data from different animals belonged to different investigations, it may be that the discrepancies observed are due to the use of different methodologies which, as stated before, can affect the results in many different ways.

## 1.6 Aims of the study

Based on what has been stated above, this project will focus on three main aims:

### **a. Validation of a method to stain the capillary, to visualize and quantify the vessels in diving mammals**

In the past years, several techniques have been used to stain capillaries (Čebašek et al., 2004) but, as already described, they seem to be affected by different factors, possibly leading to inconsistent results. After a detailed analysis of different staining technique, it was decided to apply in this project the anti-Coll-IV immunostaining method that was previously proved to be reliable in different species (Madsen and Holmskov, 1995; Weber et al., 2008; Zhang et al., 2014; Morland et al., 2017). For the quantitative analysis, the images obtained from the stained

sections were subjected to two different quantification methods. A comparison between the results obtained with the two methods and an evaluation of their accuracy will be given.

**b. Investigate whether the diving mammals' brain shows higher capillarization, when compared to non-diving mammals, as a general adaptation to hypoxia**

Evidences from previous studies suggest that, as a consequence to the exposure to hypoxic conditions, several tissues respond by increasing their level of capillarization (LaManna et al., 1992; Boero et al., 1999). Based on this and also on previous findings (Kerem and Elsner, 1973; Glezer et al., 1987; Ludvigsen, 2010), a second aim of this project is to verify if diving mammals show higher capillarization of brain tissue than non-diving mammals.

**c. Determine whether there are different levels of capillarization in different brain regions**

Several studies reported regional differences in capillary densities in the brain (Klein et al., 1986; Zeller et al., 1997; Cavaglia et al., 2001) and a strong correlation was found between the density of capillaries and the local blood flow and glucose utilization (Klein et al., 1986; Zeller et al., 1997). Because of this, this project is also focused in finding if there is any diverse level of capillarization in different cerebral regions that can be related to different degrees of hypoxia tolerance in both diving and non-diving mammals.

To pursue these objectives, the brains of two species of diving mammals, the hooded seal (*Cystophora cristata*) and the harp seal (*Pagophilus groenlandicus*), and one species of terrestrial mammal, the reindeer (*Rangifer tarandus*), were investigated.

## 1.7 Hooded seal

The hooded seal (*Cystophora cristata*) is a pinniped species that belongs to the true seal family (Phocidae). This species shows a strong sexual dimorphism with the males nearly twice as heavy as females: on average, males can reach a length between 2.5 - 2.7 meters and a weight of 300 - 400 kg, while females can reach 2.2 meters in length and around 200 kg in weight (Kovacs and Lavigne, 1986; Blix, 2005).

Their distribution is mainly concentrated in the central and western North Atlantic Ocean: from waters off Newfoundland in the south-west, to the waters around Svalbard in the north-east,

including waters around west and east coasts of Greenland (Kovacs and Lavigne, 1986; Folkow et al., 1996). They usually breed on the sea ice and two main breeding stocks have been reported: one east of Newfoundland and one between the east coast of Greenland and Jan Mayen (Kovacs and Lavigne, 1986; Folkow et al., 1996).

Pups are extremely precocial: the lactation period lasts for about 4 days and it is the shortest known not only for pinnipeds but for any mammal (Bowen et al., 1985; Kovacs and Lavigne, 1986). The lanugo fur, which is a coat of fur that offers prime insulation to the pups, is shed in utero and birth takes place on the ice during March-April. Pups usually weight between 25-30 kg and, by the time they are weaned, they can reach 42 kg (Bowen et al., 1985).

Hooded seals are expert deep-divers: even though they mainly perform meso/bathypelagic dive at 100-600 m depth, dives deeper than 1600 m have been recorded (Folkow and Blix, 1999; Andersen et al., 2013). The mean dive durations reported is between 13.5 – 14.5 minutes, with a maximum duration of 57.25 minutes (Andersen et al., 2013)

## 1.8 Harp seal

The harp seal (*Pagophilus groenlandicus*) is a pack-ice breeding phocid seal that inhabits the North Atlantic and Arctic Ocean (Sergeant, 1973; Lydersen and Kovacs, 1993; Folkow et al., 2004). Harp seals are medium-sized phocids. Adult of both sexes are similar in size: about 1.8 m long and they reach 130 kg ca. in weight (Kovacs, 2015).

They are the most abundant pinniped species in the northern hemisphere (Kovacs, 2015). Their distribution range extends in all the North Atlantic, Arctic Ocean and shelf seas: from the Hudson Bay to the west coast of Greenland, continuing east to Iceland until northern Norway and the White, Barents and Kara Seas (Sergeant, 1991). The entire population is divided in three management stocks: the Northwest Atlantic, the Greenland Sea and the White Sea/Barents Sea stocks (Sergeant, 1991; Folkow et al., 2004).

Greenland Sea harp seals usually gather into breeding aggregations on the pack ice North/North-West of Jan Mayen, where they give birth between mid-March and early April (Folkow et al., 2004). Newborns weigh about 10 kg and they gain about 2 kg/day during the nursing period that is of approximately 12 days (Kovacs and Lavigne, 1985; Blix, 2005). Pups are born with an insulating white lanugo that they completely shed during the post-weaning fast (Kovacs, 2015).



Compared to the hooded seal, the harp seal is a shallower diver (Folkow et al., 2004; Kovacs, 2015). Most of the dives do not exceed 100 m of depths, but also deeper dives up to 568 m have been recorded (Folkow et al., 2004; Nordøy et al., 2008). Most of the dives last for 5-10 min and very few of them persist until 15 or 20 minutes (Folkow et al., 2004; Nordøy et al., 2008).

## 1.9 Reindeer

The reindeer (*Rangifer tarandus*) is an arctic herbivore with a circumpolar distribution. It occurs between 50° and 81° of latitude from the northwestern U.S., Alaska, Canada, Greenland, Norway, Finland, Russia and Mongolia (Gunn, 2016). *Rangifer* is divided in 12 different subspecies which vary in size and coloration. Being a terrestrial mammal, the reindeer is less likely to experience severe hypoxic conditions than diving species.

Reindeer are migratory animals: in Scandinavia they usually undertake annual migrations from inland, where they spend the winter, to the coast in the spring (Blix, 2005). Such long migrations require a high level of activity and O<sub>2</sub> consumption, making it reasonable to assume that the animal is temporarily hypoxic and in need of higher O<sub>2</sub> uptake and delivery.

In a study by Geiseler et al. (2016) it was shown that hippocampal slices from reindeer's brain showed little tolerance to exposure to severe hypoxia in contrast to the high resistance displayed by hooded seal's hippocampal slices. The reindeer's slices had a response similar to the mice's slices, therefore the intrinsic hypoxia tolerance observed in the hooded seal couldn't be related to differences in size (Geiseler et al., 2016).

Because of the similarity between body and brain mass of seals and reindeer and also because of the possibility to have access to reindeer specimen at the Department of Arctic and Marine Biology (AMB) – University of Tromsø (UiT), the reindeer was chosen as a model of non-diving mammal for comparison.

## 2. Materials and methods

### 2.1 Animals

Table 1 shows a summary of all the animals that were used in this project.

Two adult lactating females harp seal (*Pagophilus groenlandicus*) (ID: G8 -18; G15-18) and one lactating female hooded seal (*Cystophora cristata*) (ID: K6-18) were captured in their breeding colonies on the pack ice of the Greenland Sea, at  $\sim 71^{\circ}\text{N}$  and  $\sim 019^{\circ}\text{W}$ , during a scientific cruise on the R/V Helmer Hanssen in late March 2018. During the cruise only a limited number of animals were available to be subjected to the following methodology because of other research and teaching interests, and that is why the specimen number is quite limited.

Species	ID	Date of capture/death	Age (years)	Body Mass (Kg)
<i>P. Groenlandicus</i>	G8-18	28/03/2018	7 (ca.)	114,50
<i>P. Groenlandicus</i>	G15-18	29/03/2018	unknown	121,40
<i>C. Cristata</i>	K6-18	29/03/2018	unknown	136,50
<i>R. Tarandus</i>	#10/10	04/05/2018	8	65
<i>R. Tarandus</i>	#9/10	21/09/2018	8	65

**Table 1.** Summary of the ID, date of capture/death, age and body mass of the animals involved in the project.

The two harp seals were live-captured on the ice by the use of hoop-nets and then brought on board of the vessel, where they were anaesthetized by an intramuscular injection of 2 ml of Zoletile Forte Vet (100 mg/ml, Virbac, FR). 13 minutes after the injection, a catheter was put into the extradural vein (e.d.v.), and 5 ml of heparin (5000 units/mg) were injected to prevent the formation of blood clots. Once the heparin was mixed with the blood (5 minutes ca.), a euthanizing dose of 11 ml of pentobarbital (400 mg/ml) was injected. About 30 minutes after

the injection of the anaesthetic, the dead animals were decapitated. Instead of being captured alive, the hooded seal was shot from the vessel. Since the gunshot had not made visible damage to the head (the animal was hit in the neck), this specimen was opportunistically employed for head fixation but without going through the euthanasia and heparization procedures described above. The subsequent procedures were, however, followed for all three animals.

The heads were positioned in a bucket and the carotid arteries were located on both sides of the head and cleaned from the surrounding tissues (mostly connective tissue) by use of surgical scissors. Once all the adjacent tissues were removed, the arteries extremities were kept open for the insertion of plastic tubes (5 mm diameter). In order to have a secure attachment of the tubes to the arteries, a knot was tie with a twine around the vessels and it was closed only after the insertion of the tubes. The other end of the plastic tubes was connected to plastic bottles filled with phosphate buffer 1xPBS (0.05 M  $\text{NaH}_2\text{PO}_4$ , 0.137 M NaCl, pH = 7.4) used to rinse out the blood from the head. Care was taken that the tubes were completely filled with liquid and did not present any bubbles in order to avoid the blood vessels to be filled with air. The mean arterial perfusion pressure corresponds to about 95-100 mmHg and, since a vertical column of blood exerts about 10 mmHg of pressure every 13 cm of height (Hill et al., 2012), the plastic bottles used during the perfusion procedure were maintained at a height approximately 130 cm in order to give the right perfusion pressure.

Later, the heads were moved to another bucket and the same procedure was used to start infusing the fixative, 4% paraformaldehyde (PFA [60g/1500 ml PBS]; pH = 6.9) in 1xPBS. The 4% PFA was prepared under a fume hood in the Amundsen Laboratory at the AMB, UiT, according to the following procedure: 60 g of PFA powder (P6148, Sigma-Aldrich, Germany) were diluted in 1200 ml of 1xPBS and then heated up to 60°C; once this temperature was reached, 1 N sodium hydroxide (NaOH) was added to clear the solution; when the solution looked limpid enough, 1xPBS was added to adjust the volume to 1500 ml. The solution obtained was then filtered with circular filter paper (diameter = 18.5 cm; Ashless 42, England). The procedure was repeated until a total volume of 10 lt of 4% PFA was obtained and the pH was adjusted to 6.9 by adding NaOH (1 N). Approximately 3.5 lt of 4% PFA were used to rinse each head. During the perfusion of the hooded seal's head, physiological saline solution (0.9% NaCl B. Braun) was used in addition to 1xPBS. Afterwards, the heads were completely immersed in the fixative and stored in closed buckets for about 1 week, until they were transported to the laboratories of AMB, UiT.

Two reindeer (*Rangifer tarandus*) (ID: #9/10; #10/10) from the animal facility of AMB, UiT, were also used in this project.

The reindeer #9/10 was deeply anaesthetized by the injection of 1 ml of medetomidine (10 mg/ml). 17 minutes after the giving of the anaesthetic, a catheter was put into the jugular vein and 5 ml of heparin (5000 units/mg) were injected. The euthanizing dose of 13 ml of pentobarbital (200 mg/ml) was given 8 minutes after the heparin injection. About 28 minutes after the injection of the first anaesthetic the animal was decapitated. The tissues were perfusion fixed following the same procedure described for the seals: the head was perfused with 1xPBS through plastic tubes connected to the carotid arteries; 10 minutes ca. after the decapitation the infusion of the fixative 4% PFA was started. The head was then stored in a bucket for 3 days at 4°C before the removal of the brain.

The reindeer #10/10 was opportunistically sampled after being acutely euthanized because its calf died during parturition and got stuck in the utero. The animal was shot through the brain and it was not possible to proceed with the perfusion fixation. Instead, slices of brain tissue of approximately 1 mm thickness were cut out about 10 minutes after the death and then directly immersed into the fixative, 4% PFA.

Procedures were employed with the permit of the Norwegian Food Safety Authority (#12268) and the permit to euthanize the seal was issued by Greenland and Danish Authorities.

## 2.2 Tissue sampling

After perfusion fixation, the brains were removed and stored in 0.4% PFA to avoid overfixation and antibodies destruction: since the seals heads needed to be brought from the West Ice to Tromsø, the brains were stored in 0.4% PFA about 1 week after the perfusion fixation; the brain of the reindeer #9/10 was stored 3 days after the perfusion fixation. Samples of approximately 0.5x2x1 cm were collected from different brain regions: the frontal cortex (FC) and the visual cortex (VC), including both grey and white matter, the hippocampus (HC), the cerebellum (CB) and the medulla (MED) (Figure 2). Because of tissue damages, it was not possible to collect samples of the HC from the reindeer #10/10. Each sample was placed in a vial containing 0.4% PFA and stored for approximately 1 week.

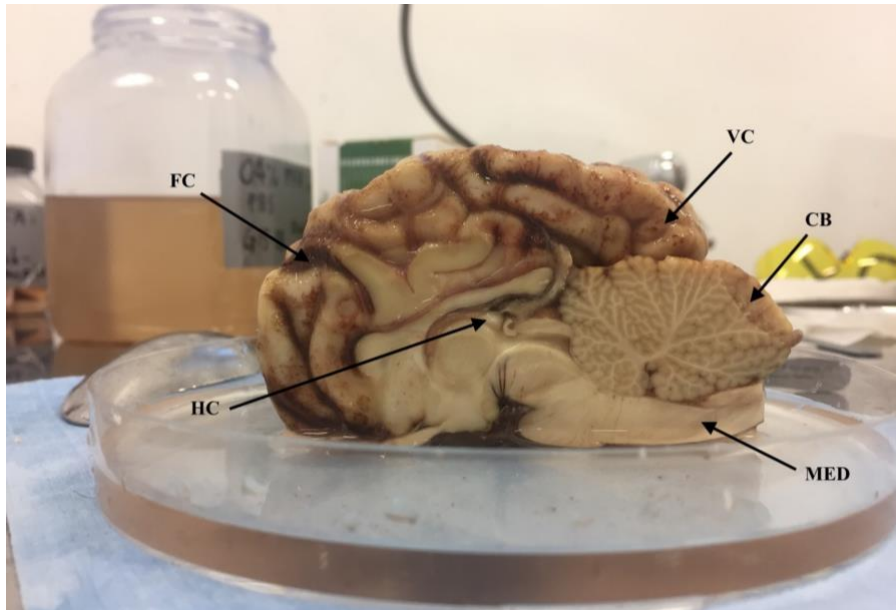


**Figure 2.** Right hemisphere of harp seal (G15-18). The arrows are indicating the regions that were sampled: frontal cortex (FC), visual cortex (VC), cerebellum (CB), hippocampus (HC) and medulla (MED).

### 2.3 Sectioning

Sectioning and staining took place at the Department of Pharmaceutical Bioscience, University of Oslo (UiO). After cryoprotection by immersion in 30% sucrose in 0.1 M sodium phosphate buffer NaPi (0.081 M Na<sub>2</sub>HPO<sub>4</sub>, 0.019 M NaH<sub>2</sub>PO<sub>4</sub>, pH = 7.4) for 24 hours ca., 0,5-cm-thick subsamples (8x4 mm) were cooled to - 40°C on a freezing microtome (Micron HM 450, Thermo Scientific) and transverse 20-µm-thick frozen sections were cut at - 20°C.

A problem that often occurs with cutting frozen sections is the formation of “freezing artifacts” that appear like abnormal vacuoles in the tissue (Rosene et al., 1986). The cryoprotection procedure is necessary for the protection against these freezing artifacts: the sucrose acts as a penetrating cryoprotective agent that infiltrates in the tissue and protects the cells against injuries from freezing (Meryman, 1971; Rosene et al., 1986). The infiltration is considered to be successful when the tissue block has sunk (Rosene et al., 1986). During the cryoprotection procedure it was noted that the grey matter was infiltrated faster than the white matter: samples with a higher ratio of grey matter sunk earlier on the bottom of the vial. Accordingly, MED samples remained floating on the top of the 30% sucrose solution even 48 and 72 hours after the immersion. It has been shown that the white matter and the grey matter have a different lipid composition (Veloso et al., 2011). Particularly, the white matter shows a higher lipid content when compared to the grey matter (O’ Brien & Sampson, 1965). The hydrophobicity

of the lipids and the lower density of the white matter could make this matter less likely to be infiltrated by the sucrose solution.

The sectioning of the FC, VC and CB was made from sections from the outer part of the cortex. By contrast, sections from the MED were obtained by cutting the central portion of the samples (Figure 3).

Since the sections were first saturated with sugar and then left free-floating in buffer, the conditions were favourable for bacterial growth. In order to avoid this, the free-floating brain sections were stored in NaPi pH 7.4 containing 0.05% sodium azide ( $\text{NaN}_3$ ) at + 5°C.

As well as in the cryoprotectant solution, MED samples were noted to be still floating more than the other sections even when stored in the  $\text{NaN}_3$  solution.

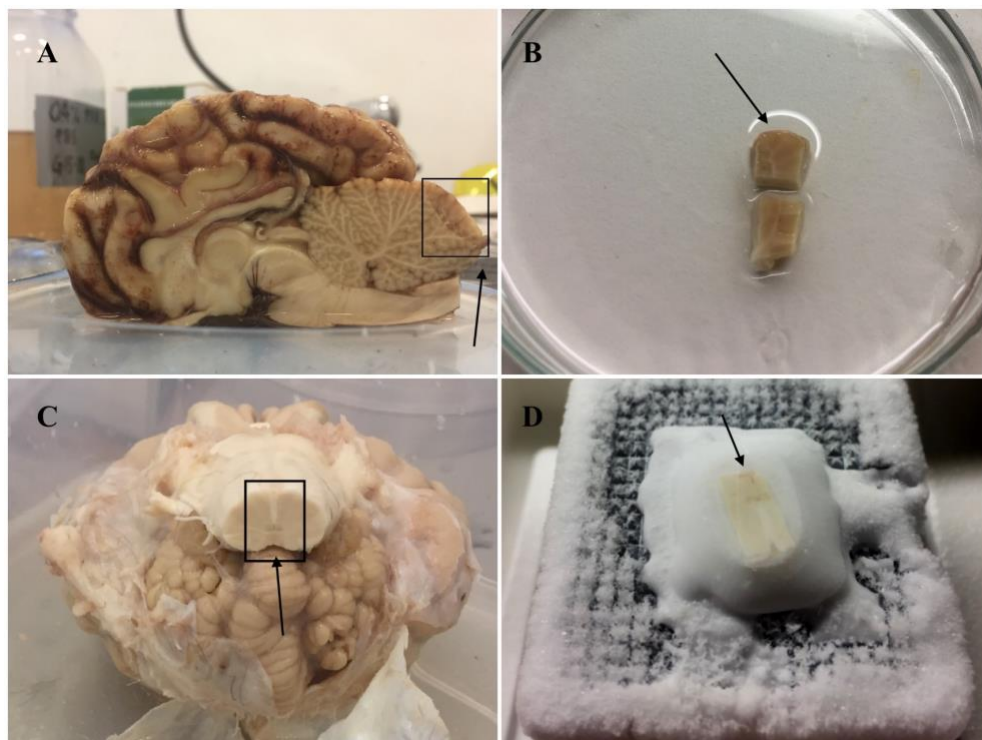


**Figure 3.** *A) Right hemisphere of harp seal (G15-18) brain. The square is indicating the region of the CB where the sample in B was collected. B) Sample of harp seal (G15-18) CB. The arrow is indicating the portion that was used as subsample for sectioning. C) Bottom and back view of reindeer (#9/10) brain. The square is surrounding the portion of the MED that was sampled. D) Subsample of the central region of reindeer (#9/10) MED positioned on the freezing microtome.*

## 2.4 Immunostaining

Antigen retrieval: the free-floating brain sections were placed in 25 well plates, each well containing 1 ml citrate buffer (0.1 M, pH = 6.5) were prepared. The plates were then incubated in a heating bath (Lab Companion, Model BW-20B) and heated up to 80°C for 30 minutes for antigen retrieval. This is a high-temperature heating method used to recover the antigenicity of tissue sections (Shi et al., 2001). Indeed, when aldehyde fixations are used, the cross-linking of proteins leads to masking of the antigen sites and this leads to a weaker immunohistochemical staining. The antigen retrieval process serves to break protein cross-linking and unmask the antigen sites. The overall strategy is to improve the staining intensity of the antibody in fixed tissues (Alturkistani et al., 2016).

Primary antibody: sections were let cool down for 20 minutes, and then rinsed with 900 µl of PBS (pH = 7.4) 2 times for 10 minutes. Unspecific binding sites were blocked by incubating the sections with 900 µl of Blocking Solution (BS) containing 1% bovine serum albumin (BSA) and 3% newborn calf serum (NCS) in PBS with 0.05% Triton X-100 (PBST) on an orbital shaker (Bel-Art™ SP Scienceware™ Spindrive™ Orbital Shaker Platform) for 2 hours. Afterwards, the sections were incubated with the primary antibody for the labeling of the vascular basement membrane. For this purpose, the sections were incubated overnight with a primary antibody (rabbit anti-collagen IV, Abcam; ab6586; diluted 1:200 in BS [5 µl/ml]) on an orbital shaker.

Secondary antibody: the day after, the sections were washed 6 times for 10 minutes with 900 µl of PBS and then incubated with the secondary antibody (goat anti-rabbit, Alexa Fluor 555, code A21428, Thermo Fisher Scientific, diluted 1:500 in BS [2 µl/ml]) on an orbital shaker for 2 hours.

Sections were rinsed again with 900 µl of PBS 3 times in 5 minutes and then incubated with 200 µl of DAPI (4',6-Diamidino-2'-phenylindole dihydrochloride, 10236276001 - Roche, Sigma-Aldrich, diluted 1:5000 [0.2 µl/ml]) in PBS for 15 minutes to stain cellular nuclei. Next, the sections were rinsed again 3 times in 10 minutes with 900 µl of PBS. Finally, the sections were moved on microscope slides and distended on it using water and a small brush. Using ProLong Gold antifade reagent (code P36930; Thermo Fisher Scientific), a cover glass was placed above the sections that were then stored overnight in a fridge at 3°C.

Negative controls were prepared by using sections from the FC (#10/10, K16-18) and the VC (#9/10, G15-18). These sections were subjected to the same procedure with the exception that they were not incubated overnight with the primary antibody but only BS instead. The negative controls were later visualized at the confocal microscope (Zeiss LSM780) to verify that no staining occurred in the absence of the primary antibody. This procedure is needed to confirm that the secondary antibody binds only the structures where the primary antibody is attached.

## 2.5 Confocal microscopy

The slides were transported back to UiT, Tromsø, to be visualized at the confocal microscope (Zeiss LSM780) in the Advanced Microscopy Core Facility (AMCF), Department of Medical Biology, Faculty of Health Science.

Large differences in capillary density exist between grey and white matter, with the grey matter having higher levels of vascularization than the white matter (Weiss et al., 1982; Klein et al., 1986; Cavaglia et al., 2001). To further investigate these differences, images at 10x magnification (2000x2000 resolution) of the 20- $\mu\text{m}$ -thick sections were acquired for all the cortical thickness (grey matter) and the white matter. Two functions were used to obtain the images: the tile-scan function, which records a defined number of adjoining single images of the sample analysed ([www.leica-microsystems.com](http://www.leica-microsystems.com)), and the z-stack function, that gives a Z-series (or Z-stack) which is a sequence of optical sections collected at different levels from a specimen (Paddock, 2000) (Figure 4 – a; Figure 18 in Appendix I too see how the optical sections appear in series).

For each image approximately 13 optical sections were obtained and the distance between them was 1.57  $\mu\text{m}$ . Two colour channels characterized each image: a DAPI channel in which the DAPI staining was visible and a second channel, in which the capillary immuno-staining was visible (Figure 5). From every image, three replicates 300x300  $\mu\text{m}$  (270000  $\mu\text{m}^2$  in total) of both grey and white matter were selected on the DAPI channel to avoid any possible bias and then analysed. In the same way, pictures of the entire cerebellar cortex and white cerebellar matter were taken.



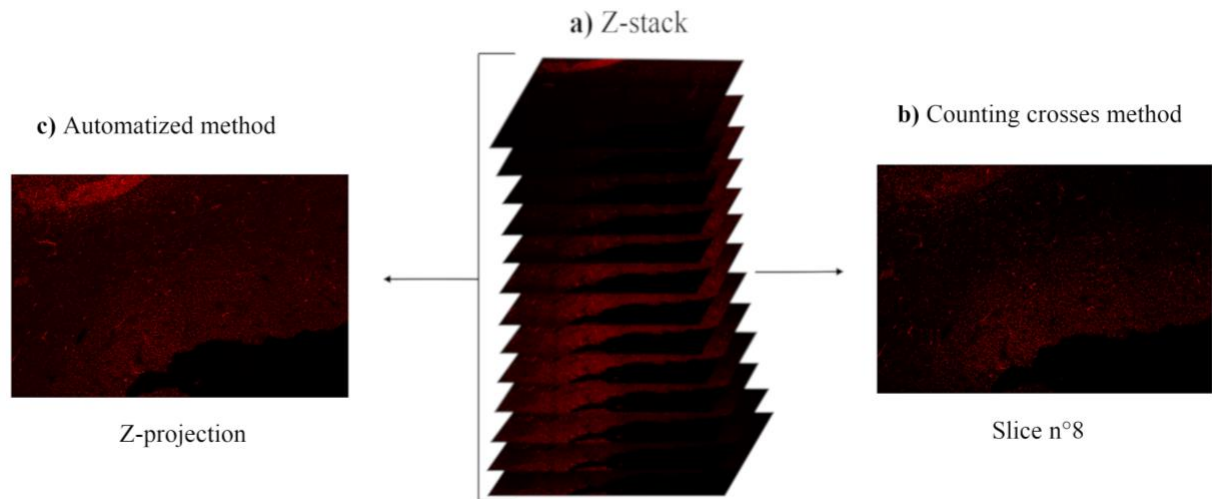


**Figure 4.** The series of optical sections obtained for VC of the hooded seal (K6-18) and how it was processed with the two different method is here illustrated. **a)** Illustration of how the Z-stack was obtained: 13 optical sections were taken from the top to the bottom of the specimen at a distance of  $1.57\mu\text{m}$  from each other. **b)** With the “counting crosses method” only one of the optical sections was picked and analysed. Particularly, from this sample the slice n°8 was chosen. **c)** The “automatized method” was instead applied to the Z-projection, which is obtained by overlapping all the 13 optical sections of the Z-stack. Only the second channel with the anti-Coll-IV staining is here illustrated.

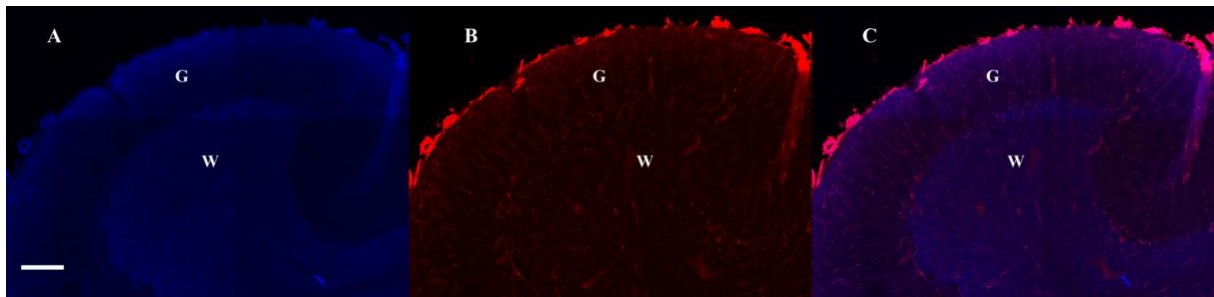


**Figure 5.** Picture of the CB of a harp seal (G15-18) obtained at the confocal microscope. The three images are represented as Z-projections of the 13 optical sections that compose the picture. **A)** DAPI channel. Here the difference between the grey (G) and white (W) matter is more visible. **B)** Second channel. The anti-Coll-IV staining is here visible. **C)** Composite image in which both channels are represented. Scale bar,  $200\mu\text{m}$ .

Since different hippocampal sectors/regions are known to display different hypoxia sensitivity (Schmidt-Kastner and Freund, 1991; Schmidt-Kastner, 2015), replicates of the CA1, CA3 and dentate gyrus (DG) were acquired (Figure 6).

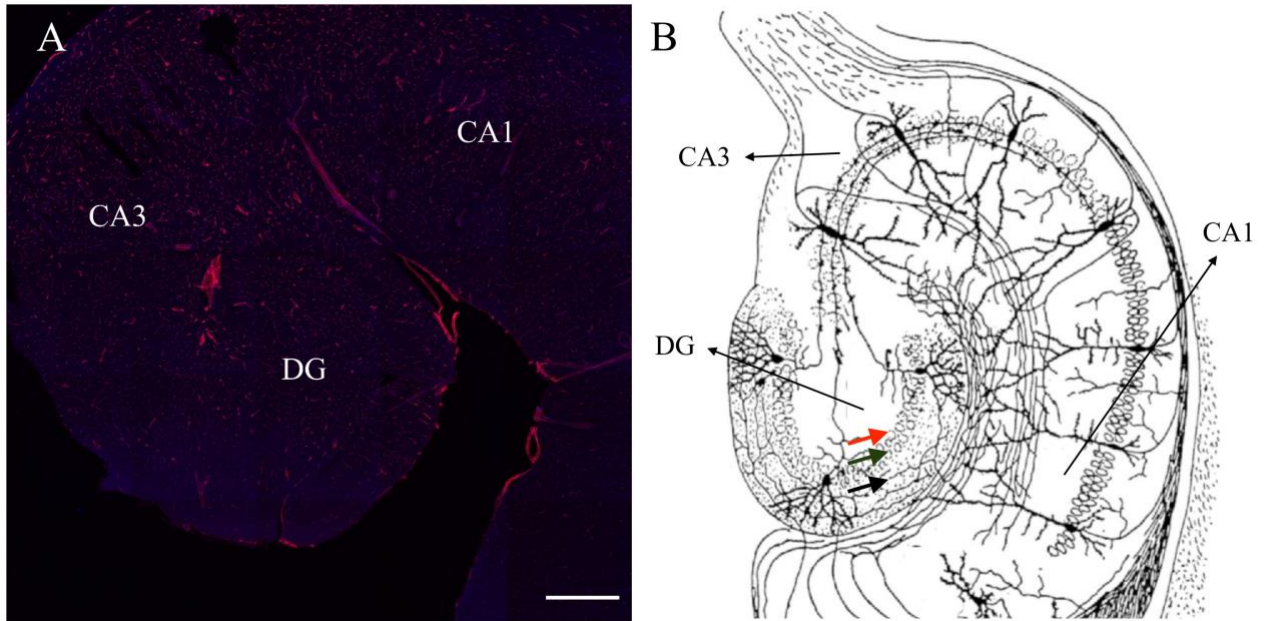


**Figure 6.** A) Composite image of the HC of one harp seal (G15-18) indicating where the different sectors CA1, CA3 and dentate gyrus (DG) are located. Scale bar, 500  $\mu\text{m}$ . B) More schematic view of the HC. Image taken from Cajal (1911) and modified in GIMP-2.10. Red arrow = Subgranular zone (SGZ); Green arrow = Granular layer (GL); Black arrow = Molecular layer (ML).

## 2.6 Quantitative analysis

A quantitative approach is necessary to better understand the correlation between morphology and function of tissues and organs, especially in comparative and experimental studies (Mandarim-De-Lacerda, 2003; West, 2012). Structural features of organs and tissues are usually best visualized on flat (2D) images or sections of the real (3D) object, but the generation of 2D images can result in the loss of information and the relationship between what is seen in the sections and the 3D features of the tissues is not readily clear (Mayhew, 1992; West, 2012). The science of stereology is the three-dimensional interpretation of two-dimensional cross sections and it enables scientists to extrapolate structural quantities of 3D objects, like volumes, surface areas, lengths and number, by sampling and analysing the structural features present in the 2D image (Mayhew, 1992; Mandarim-De-Lacerda, 2003; West, 2012). To provide quantitative descriptions, stereology uses mathematical relationships that relate the interactions of geometrical probes, such as points, lines, areas or volumes (also called *disector*), on the sections to geometric properties in 3D space (Mayhew, 1992; West 2012). The efficiency of the method depends on generating casual encounters between the randomly sampled section and the chosen test probe that is superimposed on the section (Mayhew, 1992).

In this project, two different methods were used to carry out the quantitative analysis: the “counting crosses method” and the “automatized method”.

### 2.6.1 Counting crosses method

This method was mostly performed as described in Morland et al. (2017) and, therefore, based on the Delesse Principle (Delesse, 1847 cited in West, 2012 and in Mandarim-De-Lacerda, 2003). This states that the ratio between the partial points ( $P_P$ ) that hit the objects of interest on a section in relation to the total possible points or test-points ( $P_T$ ) probed on the section is equivalent to the ratio between partial area ( $A_A$ ) to total area ( $A_T$ ) (Mandarim-De-Lacerda, 2003; West, 2012). Therefore, it is possible to estimate the area fraction of a structure through point counting (Mandarim-De-Lacerda, 2003; West, 2012). The relationship linking the area to the ratio of points is illustrated in Figure 7.

Using the Grid plug-in in the software Fiji (SciJava applications), an array of 50x50 crosses was overlaid on every replicate (Figure 8) and, by using the “multi-point” tool, the number of points over capillaries was counted. The number obtained was then compared to the total number of points to calculate the fraction of area occupied by the capillaries in the total area of the replicate. It was decided to not analyse the entire Z-projection (the optical sections all together) and to focus the analysis on only one of the optical sections in the series (Figure 4 – b). The optical sections from the most superficial portion were not considered because of the too little staining (Figure 18 in Appendix I) or because of the presence of too much background staining that could have made more difficult the identification of the capillaries. The images that in the end were analysed and from which replicates were chosen were the ones at about half depth of the Z-stack and that showed the higher staining intensity. Results are represented as mean percentage of the area occupied by the capillaries in the replicates ( $n=3$ )  $\pm$  standard deviation (SD).

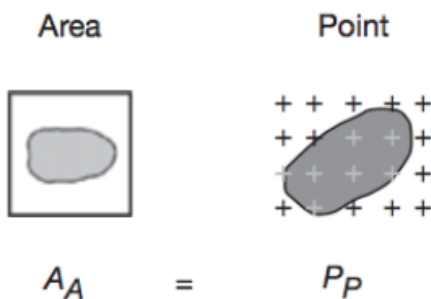


**Figure 7.** The ratio of the points hitting the profile of the object on a section to the total number of points hitting the region of interest ( $P_P$ ) is, on average, equal to the ratio of area of a sectional profile of an object to the area of the section ( $A_A$ ). (Modified from West, 2012)

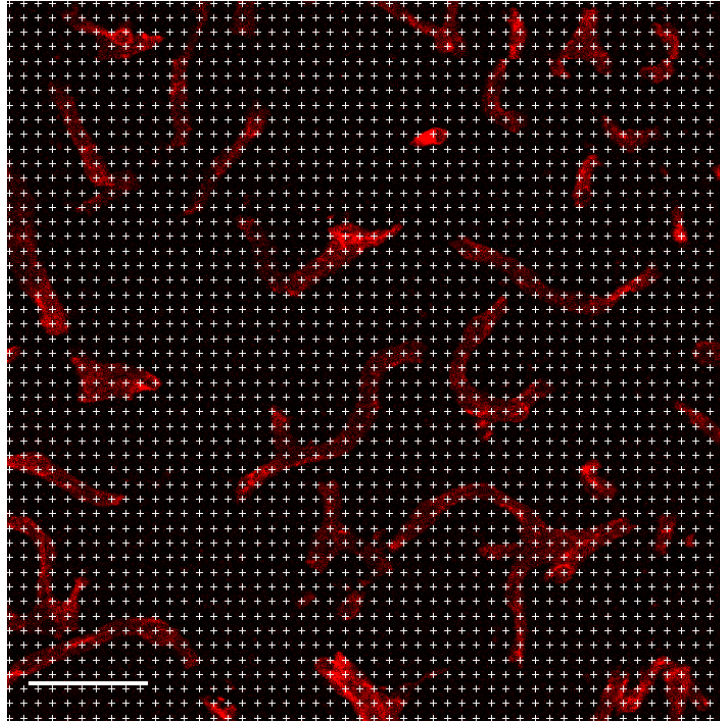


**Figure 8.** One of the 300x300  $\mu\text{m}$  replicates from the optical section n°4 of a harp seal (G8-18) FC. The figure shows how, by the use of the software Fiji, a 50x50 grid of crosses was generated on the image in order to create random encounters between the objects (capillaries – stained in red) and the probe (crosses) chosen. Scale bar, 50  $\mu\text{m}$ .

### 2.6.2 Automatized method

This method was performed through the use of a macros in the software Fiji. A macros is a programme that automatize a series of commands that can then be repeated in the analysis of several images. Two different macros were created to analyse the images (Appendix II).

The first macros (macros Step 1) was run for the entire series of optical sections of one image to create a Z-projection (Figure 4 – c) of both the DAPI and the second channel. Later, an area of about 540000  $\mu\text{m}^2$  was selected on the DAPI channel. I choose to select a bigger area (the double) than the area analysed with the “counting crosses method” in order to figure out if the “automatized method” is effectively more efficient and less time consuming. Afterwards, the second macros (macros Step 2) was run. Through this macros, in each selection the colour threshold was adjusted to pixel values 20-255 in most of the images using the Haung method (Figure 9). For some images the colour threshold needed to be adjusted to 10-255 or 30-255.

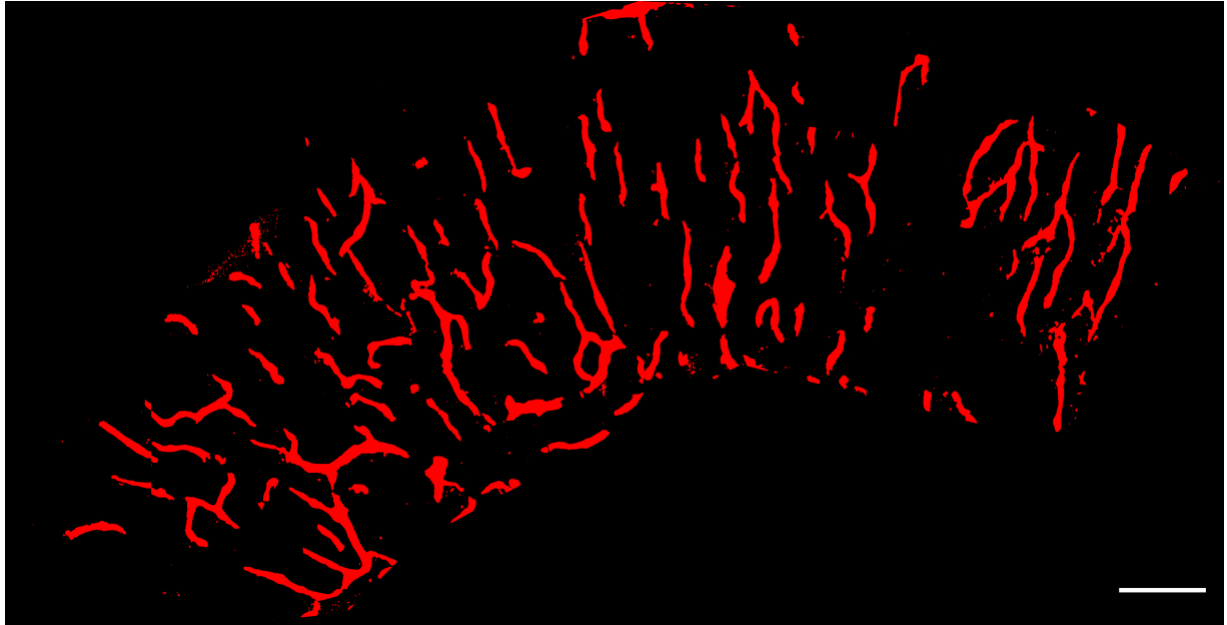


**Figure 9.** Grey matter of the CB of a harp seal (G8-18). The image shows the area selected for the application of the “automatized method” after being analysed with the macros. Scale bar, 100  $\mu\text{m}$

The colour threshold is usually used to remove parts of an image that do not fall into a specified colour range: by using this function and by running also the function “Despeckle” in the menu “Process > Noise” in Fiji, all the portions of the image that were not stained for Coll-IV were eliminated. As shown in figure 9, the final background of the image resulted in a two-colour image, making easier to recognize the stain. To avoid noise, in the Analyze menu of the software Fiji, the option “Analyze particles” was set to 10-infinity, meaning that only the objects in the image that occupied a surface equal to or bigger than 10  $\mu\text{m}^2$  were taken into account. The surface areas occupied by all the selected objects were summed together and the ratio to the total area was calculated in order to have an estimation of the surface area occupied by capillaries. All image manipulations were visually double-checked against the original picture (visible anti-Coll-IV staining) to make sure that only the capillaries were selected. Results are represented as percentage of the total area.

Using the Fiji’s tool “straight line” it was possible to measure the diameter of the vessels present in the image and, in accordance to the literature (Bell and Ball, 1985; Morland et al., 2017), only vessels with a diameter lower or equal to 10  $\mu\text{m}$  were considered as capillaries and included in the calculations. The area occupied by vessels bigger than 10  $\mu\text{m}$  was subtracted from the total area.

All the quantifications were performed blindly in regard to species and origins of the sections.

## 2.7 Statistic

A two-way ANOVA analysis and t-test were used in the software R (R Core team, 2013) for evaluating the differences in capillarization between grey and white matter, between species and regions.

Because of the low number of samples, differences between species and matter of FC, VC and CB were analysed together using the mean between replicates as values ( $n=30$ ; the values used are illustrated in Table 2 in Appendix III). For HC, differences between species and subregions were evaluated considering the means between replicates of each subregion ( $n=12$ ). The same tests were run for MED, always using the mean values between replicates ( $n=4$ ), but no significance was found. Therefore, for MED, the results will be given as mean values for each species.

Differences between regions was also assessed with a t-test (see Table 3 in Appendix III).

### 3. Results

Table 2 in Appendix III shows a summary of all the data obtained.

#### 3.1 Differences between methods

Figure 10 shows a comparison between the results obtained with the “counting crosses method” and the “automatized method”. Even though both methods gave the same results in terms of differences between diving and non-diving species and regional differences, the results obtained with the “automatized method” are, on average, higher than the ones acquired with the “counting crosses method” (see also Appendix IV). Explanations regarding such difference between the two quantification methods will be given in the discussion chapter.

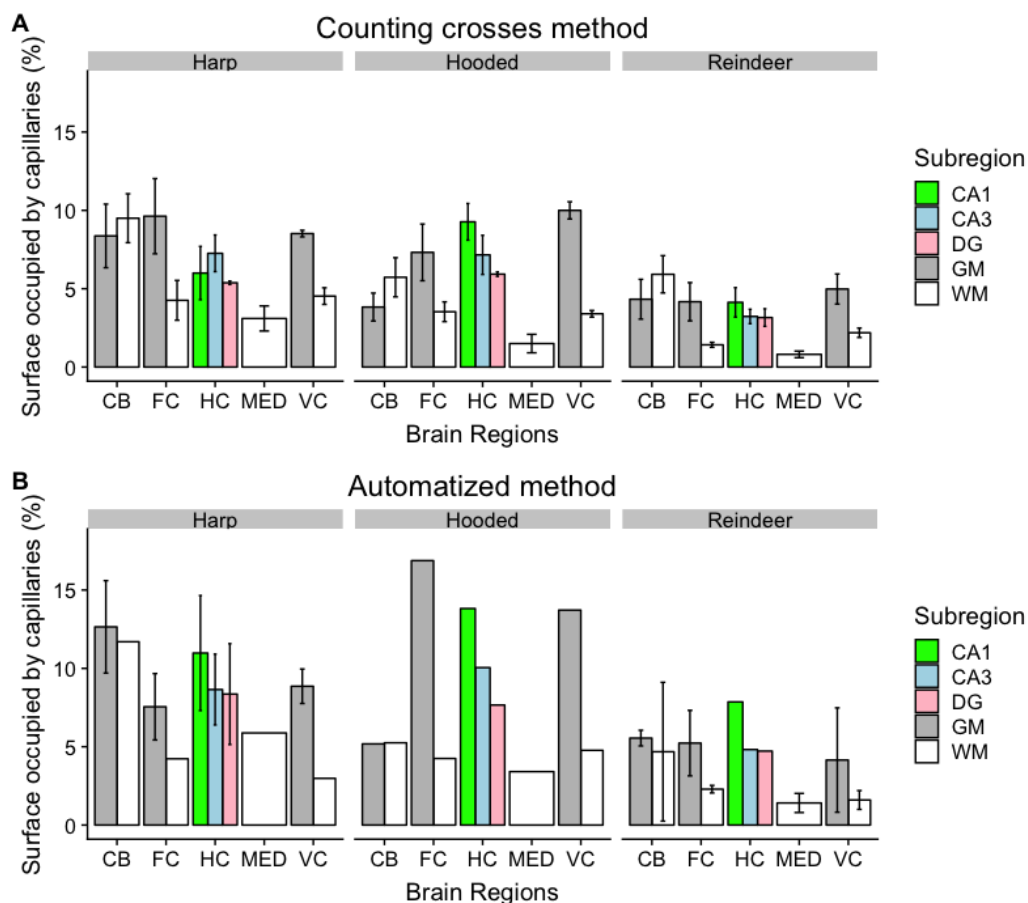


**Figure 10.** Comparison between the (A) counting crosses method and the (B) automatized method. In (A) the results are presented as mean percentage between replicates ( $n=3$ )  $\pm$  SD. Results in (B) are presented as absolute values for the hooded seal, since we had only one specimen, and as means between mean percentages ( $n=2$ )  $\pm$  SD for harp seals and reindeer since more than one individual was sampled for these two species. DG= Dentate Gyrus; GM=Grey Matter; WM=White Matter.

## 3.2 Counting crosses method

### a. Differences between species

In both cortexes (FC and VC) and CB, the diving species (harp and hooded seal) resulted to have a denser capillarization of the brain tissue compared to the non-diving one ( $p = 0.00015$ ,  $t = -4.5437$ ,  $df = 22.813$ ) (Figure 11 – A, B and C). In the MED (Figure 11 – D) capillarization levels were higher in the seals than in reindeer (mean value for reindeer: 0.81%; mean value for seals: 2.30%). A significant difference between species was also found in HC ( $p = 0.00057$ ,  $t = -5.1223$ ,  $df = 9.2604$ ), with higher values always related to the diving species.

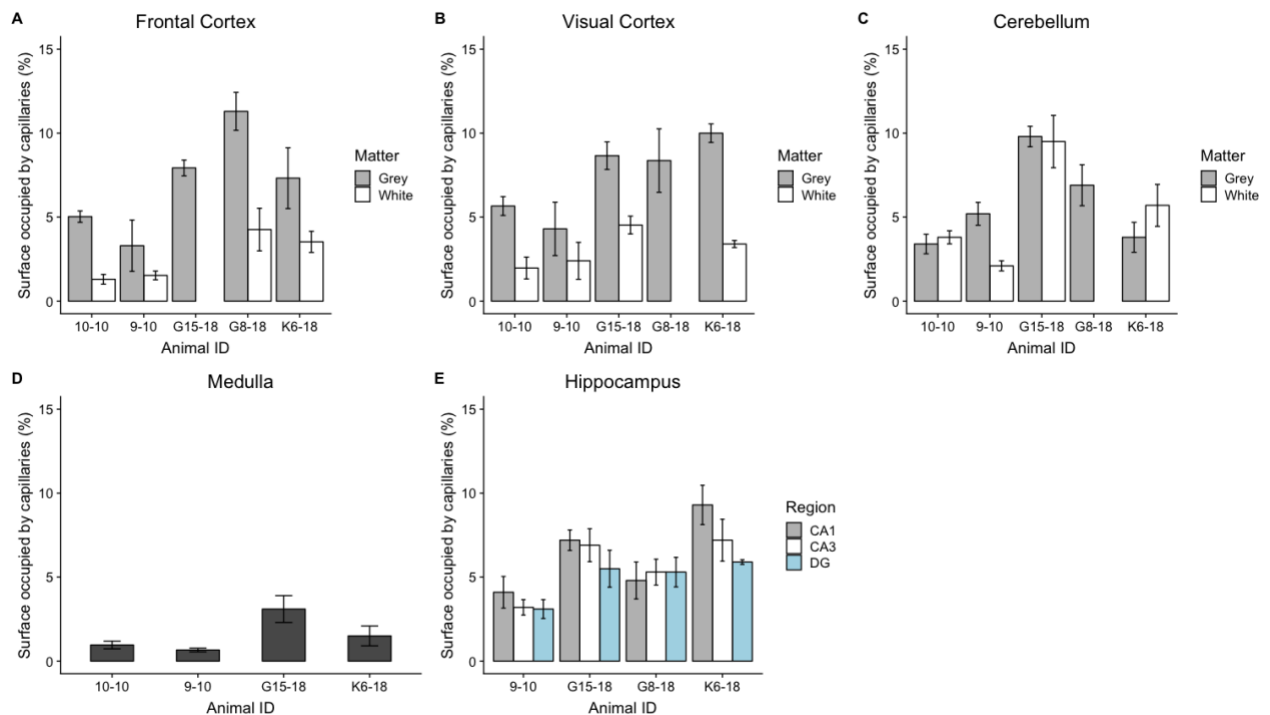


**Figure 11.** Surface occupied by capillaries in the 5 different brain regions studied in reindeer (#10-10, #9-10) and seals (harp: G15-18, G8-18; hooded: K6-18). Data were obtained with the “counting crosses method” and are represented as a mean percentage of the total area occupied by the capillaries in the replicates ( $n=3$ )  $\pm$  standard deviation (SD). **A)** Data relative to FC. Values are missing for the white matter of one harp seal (G15-18) because of complication in the individuation of this matter at the confocal microscope. **B)** Data obtained for VC. As for FC, data are missing for the white matter of one harp seal (G8-18). **C -D)** Surface occupied by capillaries in the CB and in the MED. Data are missing for the cerebellar white matter and the MED of one harp seal (G8-18). **E)** Data obtained for the HC. Hippocampal tissue of one reindeer (#10-10) was missing due to cerebral damage when the animal was shot.



b. Differences between regions

The grey matter showed higher capillarization than the white matter ( $p = 0.003$ ,  $t = 3.29$ ,  $df = 24.726$ ) in both the cerebral cortex (FC and VC) and cerebellar cortex (Figure 11 – A, B, and C). As expected, the MED was the region with the lowest percentage of capillaries (Figure 11 - D): the higher value found was  $3.1 \pm 0.8 \%$  in the harp seal G15-18.

Variations between the three hippocampal subregions did not appear to be significant ( $p = 0.34$ ) (Figure 11 - E). However, the CA1 region showed to have a consistently greater capillarization compared to the DG and the CA3 region. For all the three regions, the higher values were found in the hooded seal (K6-18, CA1:  $9.27 \pm 1.17\%$  ; CA3:  $7.16 \pm 1.25 \%$  ; DG:  $5.93 \pm 0.14 \%$ ) and the lowest in the reindeer (#9-10, CA1:  $4.13 \pm 0.94 \%$  ; CA3:  $3.23 \pm 0.46 \%$  ; DG:  $3.16 \pm 0.56 \%$ ).

Except when compared to the MED, differences between regions did not appear to be significant (Table 3 in Appendix III). More samples are needed to better assess these differences.

### 3.3 Automatized method

a. Differences between species

As in the “counting crosses method”, the seals showed higher levels of vascularization than the reindeer ( $p = 0.0021$ ,  $t = -3.4712$ ,  $df = 22.654$ ) in both cerebral (FC and VC) and cerebellar cortex (Figure 12 – A, B, and C). In the MED as well (Figure 12 – D), a higher percentage of capillaries was found in the diving species than the non-diving (mean value for reindeers: 1.41%; mean value for seals: 4.64%). Higher levels of capillarization in the diving species were found also in the HC ( $p = 0.032$ ,  $t = -2.858$ ,  $df = 5.4779$ ).

b. Differences between regions

For both cerebral (FC and VC) and cerebellar cortex, higher values of capillarization were found in the grey matter than in the white matter ( $p < 0.008$ ,  $t = 2.8831$ ,  $df = 24.815$ ) (Figure 12 – A, B, and C). The MED was again shown to be the brain region with the smallest percentage of surface occupied by capillaries (Figure 12 – D).

Differences between subregions of HC still did not appear very significant ( $p < 0.1$ ). However, the region CA1 still showed a consistently higher level of capillarization compared to the others (Figure 12 – E).

Again, no significant difference was found between regions (Table 3 in Appendix III); more samples are probably needed.

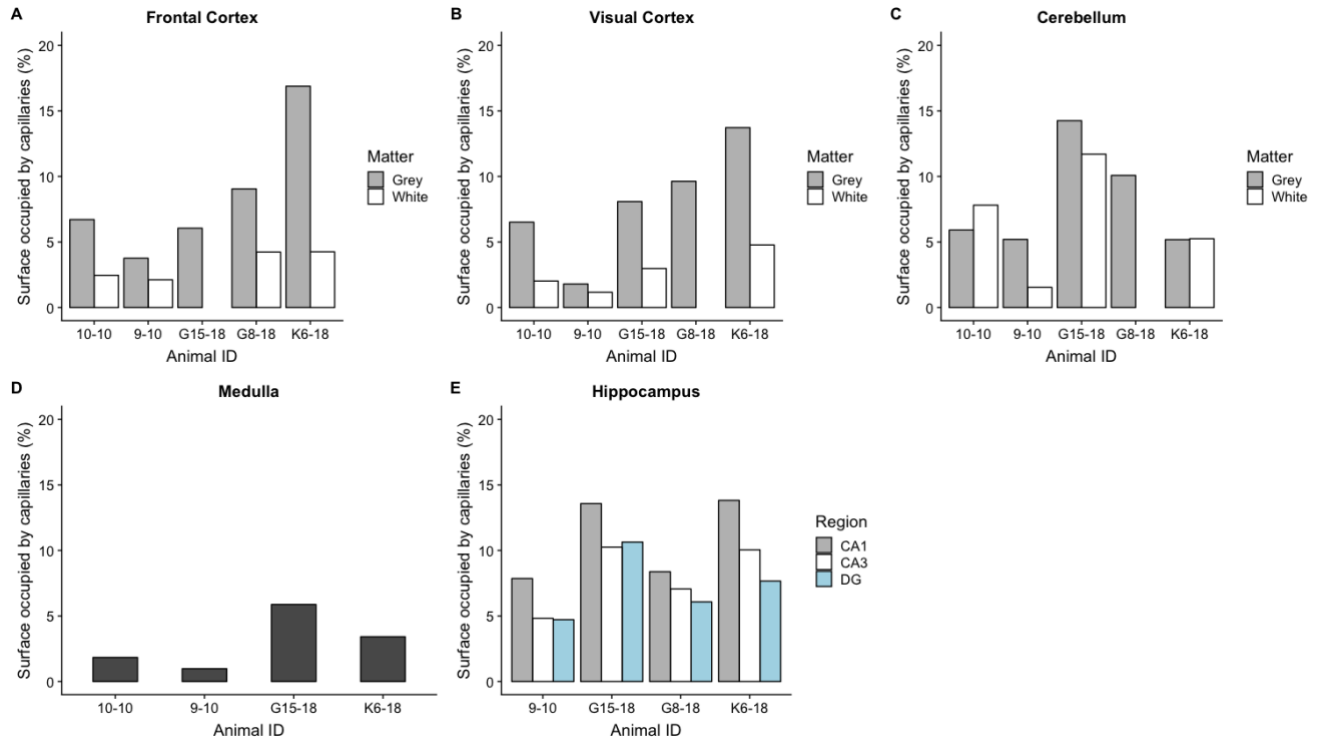


**Figure 12.** Surface occupied by capillaries in the 5 different brain regions studied in reindeer (#10-10, #9-10) and seals (harp: G15-18, G8-18; hooded: K6-18). Data were obtained with the “automatized method” and are represented as an absolute value and expressed as a percentage of the total area. **A)** Surface occupied by capillaries in the FC. Data are missing for the white matter of one harp seal (G15-18). **B)** Data relative to the VC. Information are missing for the white matter of one harp seal (G8-18). **C-D)** Data obtained for the CB and the MED. **E)** Data obtained for the three different hippocampal regions.

## 4. Discussion

Assessing the extent of capillarization of a tissue is of great importance because it is one of the parameters determining the trans-capillary O<sub>2</sub> flux (Granger and Shepherd, 1973). The latter, indeed, is a function not only of the PO<sub>2</sub> gradient between capillaries and tissue, but also of two diffusion parameters: the capillary-to-cell diffusion distance and the surface area available for the diffusion (Granger and Shepherd, 1973). These diffusion parameters are, in turn, functions of the effective capillary density (Granger and Shepherd, 1973).

### 4.1 Staining technique selection

The use of an accurate method that gives a clear visualization of the capillaries in the tissue is the necessary prerequisite to establish the capillary density in that tissue (Madsen & Holmskov, 1995; Čebašek et al., 2004). As it is shown in Čebašek et al. (2004), many attempts to stain capillaries have been done in the past years by the use of different techniques.

Several histological methods have already been used, like the toluidine blue staining (Russell et al., 1998; Ludvigsen, 2010). This method has been used to characterize the erythrocytes' cellular membranes: particularly, the toluidine blue staining binds the glycocalyx of the erythrocytes (Geyer et al., 1978, only abstract). So, the use of this staining technique for the identification of capillaries depends on the presence of erythrocytes in the vessel lumen (Čebašek et al., 2004). But, since erythrocytes are heterogeneously distributed in the microvessels, the capillaries that are not entirely perfused would be poorly recognizable and, also, the orientation of the vessels in the tissue could lead to an overestimation of the total microvascular density (Damon and Duling, 1984). To avoid these risks, it was decided to find a marker for the visualization of the vessels' wall.

Through enzyme-histochemical methods it is possible to visualize the enzyme products on the capillary wall (Čebašek et al., 2004). The alkaline phosphatase staining (Francois-Dainville et al. 1986; LaManna et al, 1992) and the amylase-periodic acid Schiff (PAS) staining (Andersen, 1975) are two examples of enzyme-histochemical methods that have already been used for the identification of capillaries.

The walls of the capillaries contain a small and relatively stable amount of glycogen. In the amylase-PAS method, the amylase digests the glycogen of the surrounding tissues in a way that

the glycogen staining does not interfere with the capillary staining (Madsen and Holmskov, 1995). After the exposure to Schiff's reagent, a mucopolysaccharide on the capillary basement membrane is mainly stained (Andersen, 1975; Qu et al., 1997), but since the amylase activity can show variations, the staining often fails (Madsen and Holmskov, 1995; Qu et al., 1997): too little amylase results in too much staining, while too much amylase will destroy the polysaccharides also in the capillary basement membrane (Madsen and Holmskov, 1995).

The enzyme alkaline-phosphatase activity is usually localized following the Gomori-Takamatsu technique (Gomori, 1939 cited in Romanul and Bannister, 1962; Takamatsu, 1939 cited in Romanul and Bannister, 1962; Gomori, 1941 cited in Čebašek et al., 2004 and in Romanul and Bannister, 1962): tissue sections are incubated in a solution containing phosphate ester and calcium ions; the activity of the enzyme produces calcium phosphate as a precipitated which is converted to cobalt sulphide to make it visible. The dark colour of the cobalt sulphide gives a measure of the enzyme activity (Davies et al., 1954). It has been shown that in the vascular tree this enzyme is located in the vessels' endothelium and it has a particularly high activity in the endothelium of capillaries and small arteries, but not veins (Romanul and Bannister, 1962; Bannister and Romanul, 1963).

Although through these methods the identification of capillaries is superior when compared to histological methods, a staining technique based on the visualization of enzyme products can lead to inconsistent results due to variations in enzyme activity or expression (Hansen-Smith et al., 1992).

The capillary wall has been successfully visualized immune-histochemically with antibodies against the endothelium itself. The von Willebrand factor (vWF) is a glycoprotein that mediates platelet adhesion to subendothelium at sites of vascular injury and it appears to be expressed exclusively on endothelial cells (Kuzu et al., 1992; Yamamoto et al. 1998). Antibodies against the vWF have been used to stain several types of tissues (Kuzu et al. 1992; Qu et al., 1997; Rufaihah et al. 2011). In a study by Qu et al. (1997), where a comparison of five different staining methods for the measurement of capillary density was made, the number of capillaries stained with the vWF method was the lowest of the five. This is due to the fact that vWF is heterogeneously expressed throughout the vascular tree, depending on the size, location and type of vessel (Kuzu et al., 1992; Yamamoto et al., 1998; Pusztasteri et al., 2006). Particularly, the microvascular endothelial cells in the brain were found to express really low levels of the vWF antigen compared to bigger vessels (Yamamoto et al., 1998).

Lectin-histochemical methods have been widely used (Alroy et al., 1987; Hansen-Smith et al., 1992; Jesmin et al., 2003). Lectins are defined as proteins that preferentially recognize and bind carbohydrates complexes protruding from glycolipids and glycoproteins (Ghazarian et al., 2011). The surface of the vascular endothelium contains specific domains with characteristic carbohydrates residues which binds different lectins (Alroy et al., 1987). The *Ulex europaeus* agglutinin I lectin (UEA-I) proved to be a more sensitive and reliable endothelium marker than vWF (Stephenson et al., 1986 cited in Qu et al, 1997). With the UEA-I method, the capillaries can be strongly stained and easily recognized (Qu et al., 1997). But, in a study by Alroy et al. (1987), in which the binding pattern of ten different lectins to vascular endothelium from ten different mammalian species was investigated, it was shown that the UEA-I stained only the human endothelium and that different lectins reacted differently depending on which mammalian tissue they were tested for.

Another immune-histochemical strategy for the staining of the capillary walls is the use of antibodies against the basement membrane (Madsen & Holmskov, 1995; Morland et al., 2017). The basement membrane is an extracellular matrix constituted by 3 opposed laminas that separate connective tissue from epithelia, endothelia, muscle fibers and the entire nervous system and, particularly, it surrounds the brain microvascular endothelial cells (Figure 1) (Bennett et al., 1959; Laurie et al., 1980; Laurie et al., 1982; Persidsky et al., 2006; Cardoso et al., 2010). Together with laminin, proteoglycans and other glycoproteins, collagen type IV (Coll-IV) is one of the major components of this extracellular matrix (Seki et al., 1998) and is the only type of collagen present in the lamina densa of the basement membrane (Stephens et al., 1982).

Antibodies against Coll-IV as a tool for the measurement of capillary density by visualizing the basement membrane in the human skeletal muscle were used for the first time by Madsen and Holmskov (1995). In that study it was shown that the anti-Coll-IV method is easy to handle and more reliable than other traditional methodologies, like the amylase-PAS method. Therefore, it was concluded that the anti-Coll-IV method can be used to determine all capillaries present in tissue sections (Madsen and Holmskov, 1995). The reliability of the use of this method in the human skeletal muscle was confirmed also by Qu et al. (1997). In more recent studies (Weber et al., 2008; Zhang et al., 2014; Morland et al., 2017) the anti-Coll-IV method was used to label the vascular basement membrane in capillaries of different brain regions of mice and monkeys.

Even though it can show variability in its efficiency depending on the species, because of its simplicity and its reliable results, the anti-Coll-IV method was chosen for this project.

## 4.2 Methodological considerations

Measurements obtained with the two different quantification methods show some discrepancies, but still they appear to follow the same trend (Figure 10). Such discrepancies are probably due to some differences in the principles that are at the basis of the two methods.

In the “counting crosses method”, the quantification analysis was performed on replicates that represented only a small fraction of the total area. Also, within the replicate, only one of the optical sections composing the image was selected in order to be analysed (Figure 4 – b). The use of only one of the optical sections and the presence of background staining may have contribute to make the identification of the capillaries much more difficult. With the “automatized method”, instead, a larger area can be studied, and the identification of the capillaries is facilitated by the absence of background staining and by the fact that the quantification is performed on the entire Z-projection (Figure 4 – c). A clear example of how these two methods can bring to different results are the values obtained for the hooded seal (*Cystophora cristata*) FC grey matter (Figure 10). By the use of the “automatized method”, a higher level of capillarization was found mostly because the quality of the image was superior after the application of the two macros in the software Fiji (Figure 13) and capillaries were selected individually through the function “Analyze particles”.

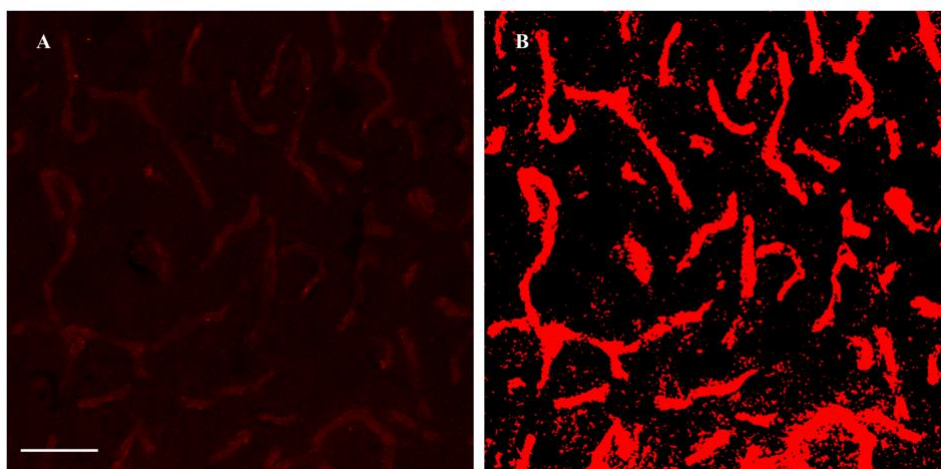


**Figure 13.** This figure shows one of the replicates 300x300  $\mu\text{m}$  from the hooded seal (K6-18) FC grey matter as obtained with **A)** the “counting crosses method” and **B)** the “automatized method”. Normally a bigger area was selected for the application of the second method, but to make a better comparative figure, the same replicate 300x300  $\mu\text{m}$  was here subjected to both the quantitative methods. Scale bar, 50  $\mu\text{m}$ .

In addition, since it allows to analyse a very large surface and, potentially, all the surface of a section, the “automatized method” does not require the use of replicates and it reduces the standard deviation (SD) to zero so, what is obtained is an absolute value without variation for each sample.

It must also be said that, hypothetically, by increasing the number of crosses that were superimposed on the replicates from 50x50 to, for example, 1000x1000, the results obtained with the “counting crosses method” might have been closer to the ones obtained with the “automatized method” because of the higher resolutions.

Another factor that should be taken into account is that the reindeer #10-10 brain was not perfusion fixed like all the other specimens, but it was immersion fixed. In a study by Beach et al. (1987) it was shown that the quality of the fixation achieved by the two methods can be different: the perfusion fixation produced more uniformly stained sections independently from the antigen studied, while in the sections that were immersion-fixed the staining was not uniformly distributed. The authors concluded that such differences were probably due to the different fixation requirements of different antigens (Beach et al., 1987). The results obtained for the reindeers that were here examined do not seem to be particularly influenced by the use of different fixation methods. By contrast, more discrepancies between the two specimens were found after comparison of the results obtained with the two methods, suggesting that the results were more affected by the quantitative method rather than the fixation method.

Overall, the “automatized method” resulted to be easier to apply to the images and less time consuming. Also, even though we had a limited sample size, it was enough to achieve our prime objective: validate an appropriate capillary staining and quantification method.

### 4.3 Differences between species

A wide number of studies, which investigated the effects of experimental, exercise-induced and altitude-related hypoxia, indicate that the exposure to hypoxic conditions can cause changes in the capillary density of a tissue (Andersen and Henriksson, 1977; Hather et al., 1991; LaManna et al., 1992; León-Velarde et al., 1993; Mathieu-Costello et al., 1998; Boero et al., 1999; Jensen et al., 2004; Cocks et al., 2013).

In 1977, Andersen and Henriksson showed that endurance training can stimulate capillaries proliferation in human skeletal muscle. The increase in capillary density was related to the

increase of the maximal O<sub>2</sub> uptake of the tissue, suggesting a relation between capillarization and oxidative capacity of the tissue (Andersen and Henriksson, 1977). The O<sub>2</sub> uptake of a tissue from the capillaries is indeed related to the mean transit time (MTT) of the erythrocytes passing through the capillaries and, MTT is in turn related to the density of capillaries in that tissue (Saltin, 1985). The enhanced capillary density results in a longer MTT, which gives optimal conditions for the exchange of gases, like O<sub>2</sub>, and a larger resistance to training (Saltin, 1985). Flight muscles of birds adapted to high altitude are also known to display enhanced capillarization (León-Velarde et al., 1993; Mathieu-Costello et al., 1998). Particularly, in the pectoralis muscles of grey crowned rosy finches (*Leucosticte arctoa*) living at 4000 m, a proportional increase was found between the ratio of capillaries per muscle fiber and the volume of mitochondria per muscle fiber (Mathieu-Costello et al., 1998). Since the mitochondria are the place where the oxidative phosphorylation occurs, those findings confirmed that an adequate level of capillarization is crucial to meet the needs of O<sub>2</sub> of a tissue, especially during stressful hypoxic conditions, like training and a life at high altitude.

Rodents' brains have been also reported to show enhanced capillarization after exposure to prolonged hypoxic conditions (LaManna et al., 1992; Boero et al., 1999). Changes in capillarization were accompanied by a shortening of the intercapillary diffusion distance and, therefore, an increase in O<sub>2</sub> diffusion conductance (Boero et al., 1999), further verifying the hypothesis that the microvascular adjustments play a key role during conditions of O<sub>2</sub> deficiency.

In hypoxic conditions, like diving, the P<sub>a</sub>O<sub>2</sub> can be reduced to very low levels (Kerem and Elsner, 1973; Qvist et al., 1986; Meir et al., 2009). An increased blood flow together with a decreased diffusion distance is what is needed to maintain an adequate O<sub>2</sub> delivery to the tissues and both these parameters are usually coupled to an increased capillary density (Granger and Shepherd, 1973; Boero et al., 1999). Facing hypoxia on a regular basis, it is possible that diving species evolved specific adaptations, like an increased capillary density, in those tissues that are particularly sensitive to the O<sub>2</sub> absence. Only few studies have been conducted on marine mammals (Kerem and Elsner, 1973; Glezer et al., 1987; Ludvigsen, 2010) but they all seem to confirm such prediction.

Kerem and Elsner (1973) found that different regions of the brain cortex of the Northern elephant seal (*Mirounga angustirostris*) had a higher number of capillaries/mm<sup>2</sup> than in other mammals, like the mouse and the cat. The results obtained from this study were reused by



Ludvigsen (2010) for a comparison between different species, including also the hooded seal (*Cystophora cristata*) and the dog. Again, the capillary density was shown to be higher in the diving species than in the others. The study conducted by Glezer et al. (1987) on the dolphin (*Stenella coeruleoalba*) did not just show a difference between species but also within the region analysed.

The principal problem with the data used for the comparisons made in these studies is that they come from different investigations, each of which used a different methodology. Therefore, the discrepancies seen may be due to the application of different staining technique or different quantification methods, whose importance is instead crucial when performing this kind of comparative studies.

In addition, the species that were compared in these investigations do not really resemble each other in body size and this may introduce also a scaling problem. Indeed, Krogh (1918) showed that, at least in muscles, the number of capillaries varies depending on the body size. The number of capillaries appeared to be also a function of the metabolism, that is known to be higher in small mammals than in larger ones. Therefore, it can be deduced that the level of capillarization of a tissue increases with decreasing body size (Krogh, 1918). Krogh's investigation resulted quite limited since it took into account only three species (horse, dog and guinea pig), but a more detailed analysis was given by Schmidt-Nielsen and Pennycuik (1961) who studied the capillary density in the muscles of ten different mammalian species, which varied very widely in body mass. Their results were in accordance with Krogh's findings: the small mammals tended to have a higher capillary density, but with increasing body size the relation found between capillary count and body mass did not appear to be as robust as expected. The authors suggested that this is due to the fact the number of capillaries may be affected by other factors, like training or altitude, as I also discussed above (Andersen and Henriksson, 1977; León-Velarde et al., 1993; Mathieu-Costello et al., 1998).

To avoid all the uncertainty related to scaling and the application of different methodologies, in this project I tried to further verify the existence of differences in brain capillary density between diving and non-diving species by studying species that have a more comparable brain size, like seals and reindeer, and by subjecting them to the same methodological procedure. Generally, my findings are in accordance with the conclusions from previous studies (Kerem and Elsner, 1973; Glezer et al., 1987; Ludvigsen, 2010), showing that the diving species have higher levels of capillarization than the non-diving species. These results add to the arsenal of

intrinsic hypoxia adaptations already documented in seals (Burns et al., 2007; Folkow et al., 2008; Geiseler et al., 2016)

The hooded seal is known to dive deeper and longer than the harp seal (Andersen et al., 2013; Folkow et al., 2004) and this is reflected by their different body O<sub>2</sub> stores: 89.5 ml/kg in the hooded and 71.6 ml/kg in the harp (Burns et al., 2007). The two species also show different blood volumes (169 ml/kg for the harp and 194 ml/kg in the hooded) and concentration of myoglobin in the muscles (86 mg/g in the harp and 94.8 mg/g in the hooded) (Burns et al., 2007). The fact that these values are all higher for the hooded seal suggests that diving behaviour is a determinant factor for the extent to which these species display adaptations to diving. If this is true, it is possible that the two species, harp and hooded seal, also show different levels of capillarization in the brain. Since only one hooded seal specimen was available, it was not possible to make a direct comparison between the two diving species, but it would be interesting to have the chance to further verify also this hypothesis.

#### 4.4 Regional differences

An appropriate level of vascularization of the tissue is fundamental for the sustainment of the metabolic activity of that tissue. Several studies have demonstrated that there is a close relationship between local glucose utilization and density of capillaries, and that variations can be seen between different cerebral regions (Klein et al., 1986; Zeller et al., 1997).

##### 4.4.1 Cerebral and cerebellar cortex

In both FC and VC, the grey matter showed a higher capillarization compared to the white matter, independently from the species studied and the method applied (Figure 11 - A and B; Figure 12 - A and B). This result is not totally unexpected if the different energy demands of the two types of matter are taken into account. The energy expenditure of the cerebral cortex grey matter was found to be 20.4  $\mu\text{mol ATP/g/min}$  (Howarth et al., 2012), which corresponds to 122.4 mmol ATP/100g/h. Assuming that for 6 ATP produced 1 O<sub>2</sub> is consumed, this will result in an O<sub>2</sub> consumption of 20.4 mmol/100g/h. The total energy use of the white matter corresponds to only 40-45% of that in the grey matter (Harris and Attwell, 2012) and, therefore, to an O<sub>2</sub> consumption of approximately 9.18 mmol/100g/h. These differences are due to the

fact that the majority of the brain's energy is used for synaptic currents and action potentials (Attwell and Laughlin, 2001; Howarth et al., 2012), but synapses are not equally distributed between grey and white matter: the density of synapses was found to be  $7.36 \times 10^{17}$  synapses/m<sup>3</sup> in the cerebral cortex grey matter of rats and  $8.95 \times 10^{15}$  synapses/m<sup>3</sup> in the developing optic nerve (Harris and Attwell, 2012). Also, the energy consumption per synapse per second is lower in the white matter than in the grey matter (Harris and Attwell, 2012). Given these two factors, it is not surprising that the energy demand and, thus, the O<sub>2</sub> consumption is lower in the white matter than in the grey matter. Such results were verified also in a study about density of microvessels in the human brain by Kubíková et al. (2018), and in the rat brain (Klein et al., 1986; Cavaglia et al., 2001).

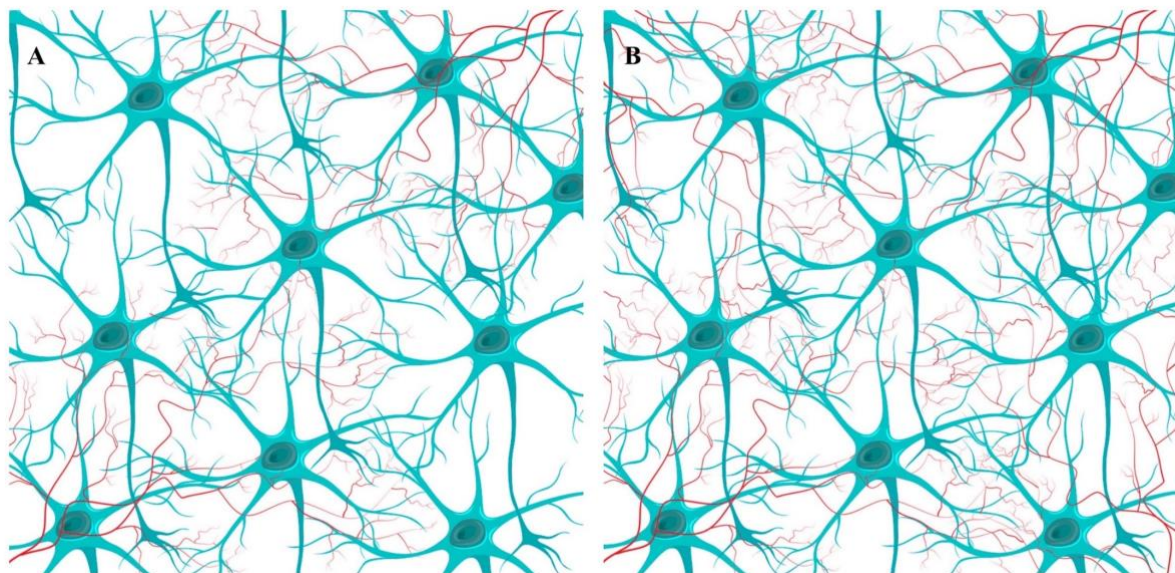


**Figure 14.** Differences between neural tissue with low (A) and high (B) levels of vascularization are here illustrated. It is clear that in the more vascularized tissue neurons can be supplied with oxygen more easily. Images were taken from <https://www.vectorstock.com/> and then modified in GIMP-2.10

One way to provide the grey matter with all the ATP that it needs to match its high synaptic activity, is to guarantee an appropriate amount of O<sub>2</sub> delivery. Brain neurons are supplied by oxygen primarily by diffusion through the capillary wall (Nicholson, 2001). The efficiency of this process depends not just on the difference in oxygen pressure between capillaries and tissues, but also on the diffusion distance (Granger and Shepherd, 1973). There is a direct relationship between capillary density and average distance between cortical capillaries: an increased vascularity reduces the intercapillary distance and increases the blood flow, improving the O<sub>2</sub>-diffusion capacity in order to give a better support of the brain metabolic

activity (Hunziker et al., 1974; Granger and Shepherd, 1973): the blood flow is able to deliver oxygen to more neurons at the same time and faster (Figure 14).

Indeed, a correlation was found between metabolic demand and capillary density in different layers of the VC of monkeys (*Macaca mulatta*) (Weber et al., 2008). This verifies the theory that the increase of the capillary density is of central importance in supplying tissues with oxygen and other energy substrates (Weber et al., 2008).

With respect to the CB, vascular differences between the grey and the white matter show some variations depending on the counting method applied (Figure 10). On average, from the results obtained with the “counting crosses method” it appears that the white matter has a higher level of capillarization than the grey matter, while the “automatized method” seems to indicate the opposite with the exception of the values obtained for the hooded seal, in which vascularization of grey and white matter appear to be very similar even after the application of the second method. But since we had very few specimens, all the results obtained should be judged with some caution.

Such discrepancy may be due to differences in the two methods: with the “counting crosses method” only small replicates 300x300  $\mu\text{m}$  were selected and analysed and, for the grey matter, replicates were chosen from the outer border of the section; with the “automatized method”, instead, the entire thickness of the cerebellar cortex grey matter was selected and analysed.

In mammals, the whole cerebellar cortex is predicted to consume 12.8  $\mu\text{mol ATP/g/min}$  (12.8  $\text{mmol O}_2/100\text{g/h}$ ), of which 57% is used in the granular layer and 43% in the molecular layer (Howarth et al., 2012). This distribution of the energy use reflects the presence of diverse types and number of cells in the different layers of the cerebellar cortex (Howarth et al., 2010; Howarth et al., 2012) (Figure 15). The Purkinje cells, that are the largest neurons present in the CB, consume  $8.19 \times 10^9$  molecules of ATP/s, while the small granule cells of the granular layer consume only  $1.32 \times 10^8$  molecules of ATP/s (Howarth et al., 2012). But, since the granule cells are present in a greater number than the Purkinje cells, the total energy consumption will result much higher for the granule cells than for the Purkinje neurons (Howarth et al., 2010; Howarth et al., 2012). Taking this into account, it is understandable that the molecular layer is consuming less energy than the granular layer.

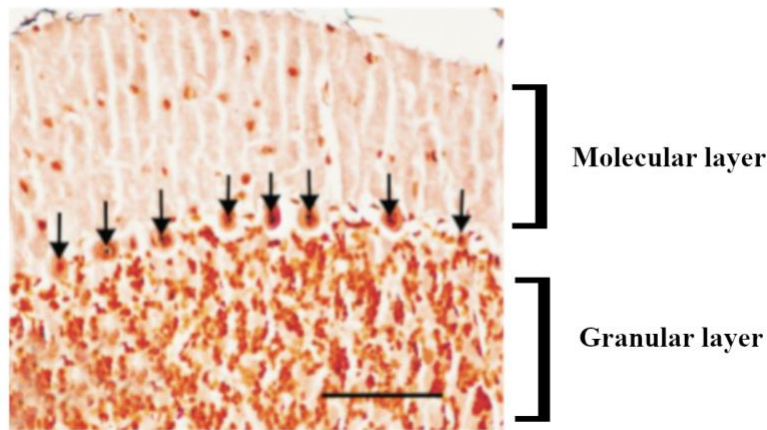


**Figure 15.** Organization of the cerebellar layers in rat brain. The black arrows are indicating the Purkinje cells. Image taken from Celik et al. (2018) and modified in GIMP-2.10. Scale bar, 50  $\mu$ m.

Since with the “counting crosses method” only the outermost part of the grey matter was selected, it is likely that just the molecular layer was analysed and, assuming that also in seals and reindeer there is a major concentration of cells in the granular layer than in the molecular layer and that only the regions that consume more energy have a denser capillarization, it is possible that the results obtained for the cerebellar grey matter with this method are an underestimation. In fact, with the use of the “automatized method”, in which the entire cortical thickness was analysed, the levels of capillarization of the grey matter were 45% higher in the harp seals and 28% higher in reindeer than with the “counting cross method”. Indeed, in a study about mice brains, Kolinko et al. (2016) showed that the granular layer and the cerebellar nuclei were characterized by the highest density of microvessels and, therefore, also by the shortest diffusion distance. This vascular arrangement reflected the high demand of energy supply of the two regions (Kolinko et al., 2016). Also, in a study by Boero et al. (1999), the granular layer was shown to be the layer with the highest length of capillaries and the lowest intercapillary distance.

However, in Howarth et al. (2012), a correlation was found between the energy use and the energy supply, in which the molecular layer seems to be the most vascularized. But the staining technique used in this study does not distinguish different types of blood vessels and, therefore, also arteriole and venule were included in the calculations (Howarth et al., 2010). This may have led to higher levels of vascularization compared to the ones obtain in this project, since we wanted to specifically quantify the surface area occupied by the capillaries, excluding any other type of blood vessels.

As stated before, the energy expenditure of the cerebral grey matter and the cerebellar grey matter have been calculated to be 20.4 mmol O<sub>2</sub>/100g/h and 12.8 mmol O<sub>2</sub>/100g/, respectively

(Howarth et al., 2012). Because of the relationship between energy demand and energy supply, the cerebral grey matter is expected to show a higher capillarization than the cerebellar grey matter. But, looking at my results this doesn't seem to be always the case (Figure 16). For the hooded seal (K6-18), the grey matter of both VC and FC seems to show a higher density of microvessels than the cerebellar grey matter, independently from the method used. The situation appears to be the same, but less marked, also for the reindeer #10-10. By contrast, looking at the results obtained for the reindeer #9-10 and the harp seal G15-18 it seems that the surface occupied by capillaries is higher in the cerebellar grey matter than in the cerebral grey matter. This trend is even more emphasized with the application of the “automatized method”. In a recent study about microvasculature of the human brain (Kubíková et al., 2018), it was shown that, on average, the cerebellar cortex had a higher density of microvessels than the cerebral cortex. But, looking at the dataset, which was separately published (Tonar, 2017), their results appear as conflicting as mine.

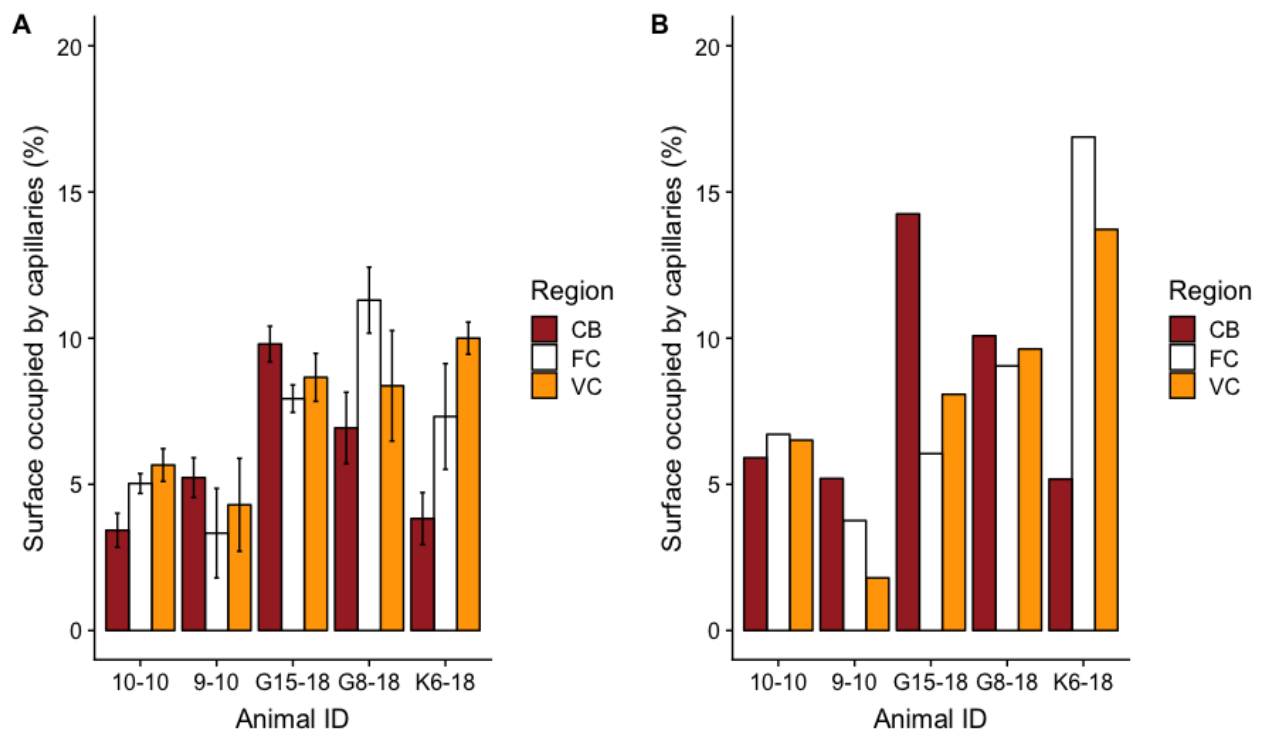


**Figure 16.** Differences in the capillarization of grey matter in frontal (FC) and visual cortex (VC) and cerebellum (CB) in each individual. **A)** Results obtained with the “counting crosses method” represented as mean percentage between replicates ( $n = 3$ )  $\pm$  SD. **B)** Results obtained with the “automatized method”.

One factor that may have influenced my results is the orientation of the capillaries in the two types of grey matter. In the cerebellar cortex, capillaries were oriented parallel to the cutting plane, while in the cerebral cortex they were mostly oriented perpendicularly. Since the results are here expressed as surface area occupied by the capillaries, it is possible that the apparent unmatched relationship between oxygen demand and oxygen supply that we see is due to the different spatial orientation of the capillaries in different regions of the brain. Probably, with a bigger number of samples we could have probably define in a better way differences between cerebral and cerebellar cortex.

#### 4.4.2 Medulla

Independently from the method used, the MED showed levels of capillarization lower than any other region (Figure 10), with only few exceptions for the white matter.

The MED is part of the brain stem, whose organization resembles the one of the spinal cord: nuclei of grey matter embedded in the white matter. Such organization is reflected by the vascular distribution that can be indirectly deduced from the study by Friede (1965) in the brain of the rhesus monkey about the activity of the alkaline phosphatase enzyme, which appear to be located mainly in blood vessels. Regional variation of the enzyme activity was detected in the MED, with the nuclei of grey matter having higher levels of activity than the white matter (Friede, 1965). The number of blood vessels/mm<sup>2</sup> in the MED was investigated also by Patt et al. (1997) but, because of the high standard deviation, it was not really easy to assess any difference with the other regions studied or between normoxic and anoxic conditions.

To my knowledge, not many studies have been performed about the levels of capillarization in the medulla and, therefore, it's not possible to make a comparison with other results.

#### 4.4.3 Hippocampal subregions

Hippocampal subregions show selective vulnerability to different kind of disturbances and, the possibility that this may be due to different arrangements of the vasculature has been debated for long (Bell and Ball, 1981; Aitken and Schiff, 1986; Imdahl and Hossman, 1986; Schmidt-Kastner and Freund, 1991; Kadar et al., 1998; Schmidt-Kastner, 2015). In a study by Kadar et al. (1998) it was shown that the CA1 region was less damaged than the CA3 region after exposure to hypobaric hypoxia, while the exposure to global ischemia caused more damages in

the CA1 than in the CA3. It was stated that this may be probably due to a different metabolic demand of the two regions and the intrinsic properties of the neurons inhabiting them, like the presence of different receptors on their membranes, etc. (Aitken and Schiff, 1986; Kadar et al., 1998). So, it is not clear if there is a relation between the arrangement of the vasculature and the sensitivity of the subregions to disturbances such as hypoxia or global ischemia (Aitken and Schiff, 1986; Kadar et al., 1998; Løkkegaard et al., 2001).

Numerous studies have been done about the organization of the hippocampal microvasculature, but their results show high variability and they do not always match with each other. In 2001, Løkkegaard et al. showed that in human HC the CA1 had the highest surface area occupied by capillaries when compared to the CA3 and the hilus of the DG. Another study by Czéh et al. (2010) in rats brain reported a higher number of capillaries in the CA1 compared to CA2-3. By contrast, in another study about rats' brain, Cavaglia et al. (2001) showed that the CA1 resulted to have a capillary density lower than both the CA3 and the hilus. Imdahl and Hossmann (1986) showed that the CA1 had a low density of perfused capillaries also in gerbil's brain.

The values obtained in this project also varied depending on the subregion studied and the tendency of such variability was preserved independently from the method used (Figure 10). Even though the sample size was not big enough to show any significant difference, on average the CA1 showed the highest percentage of surface occupied by capillaries, followed by the CA3 and then the DG, independently from the species, confirming what was found in some of the previous studies (Løkkegaard et al., 2001; Czéh et al., 2010).

Given the use of different methodologies, units of measurements and species it is difficult to assess the importance and the significance of the discrepancies that are reported in the different studies cited above. Since in my study two different species were subjected to the same staining and quantification methods, I feel confident in saying that the values found in this study both between species and between regions are quite reliable. However, more studies are needed to better clarify the microvascular organization of the hippocampus.

The DG has three principal layers (Figure 6 – B and Figure 17): the molecular layer which is occupied by the dendrites of the granule cells; the granular layer, that is inhabited by the granule cells; and the polymorphic layer, occupied by the mossy cells and that is usually referred to as the hilus (Amaral et al., 2007; Scharfman and Myers, 2013).



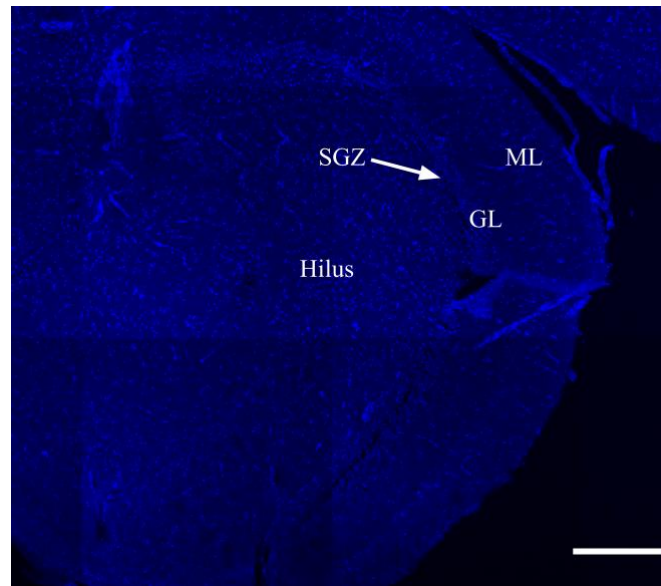


**Figure 17.** Organization of the HC (Harp seal G15-18). Only the DAPI channel is here represented. ML = Molecular layer, GL = Granular layer, SGZ = Subgranular zone. Scale bar, 300  $\mu$ m.

At the border between the hilus and the granular cell layer there is a thin lamina called subgranular zone (SGZ) (Figure 6 – B and figure 17) that, together with the subventricular zone (SVZ) of the lateral ventricles, has been demonstrated to be one of the sites in which neurogenesis takes place in the adult mammalian brain (Kaplan and Hinds, 1977; Khun et al., 1996; Eriksson et al., 1998).

The newborn neurons in the SGZ undergo several physiological and morphological stages and, once they mature, they migrate into the granule cell layer (review: Zhao et al., 2008). In a study by Palmer et al. (2000), neuronal precursors were found to proliferate together with angioblasts, which are a type of endothelial precursor cells that differentiate into mature endothelial cells and subsequently develop into blood vessels. Particularly, the new blood vessels have been shown to play an important role as scaffolds during the migration of the newly formed neurons: the two vascular ligands stromal-derived factor 1 (SDF1) and angiopoietin 1 (Ang1) act as directional factor by interacting with their receptors CXCR4 and Tie2, respectively, on the neighbouring neuroblasts (Ohab et al., 2006). It is believed that the vascular endothelial growth-factor (VEGF) can act not only as an angiogenic element, but also as a neurogenic factor (Cao et al., 2004). In the HC, VEGF is expressed both by granular cells and subgranular astrocytes and such neuronal expression of VEGF may be an important regulating factor for neurogenesis (Cao et al., 2004). Because of the strong association between neuronal and endothelial precursors it is likely that the overexpression of VEGF in response to some environmental stimuli, such as hypoxia or ischemia, may simultaneously stimulate neurogenesis and

angiogenesis (Palmer et al., 2000; Cao et al., 2004). Indeed, Teng et al. (2008) showed that, after exposure to stroke, cerebral microvascular endothelial cells of the SVZ can enhance neurogenesis and that, in turn, the SVZ cells activated by the stroke expressed high levels of VEGF, promoting the formation of capillary tubes. These findings were confirmed by a more recent study (Zhang et al., 2014) which showed that in the stroke brain, there is an increase of blood vessels (mostly capillaries) in conjunction with the process of neurogenesis.

Having this in mind, it may be surprising to see that in our results the DG was, on average, the hippocampal region with the lowest amount of surface occupied by capillaries (Figure 11 - E and 12 - E). As stated before, the process of neurogenesis in the hippocampus is circumscribed within the SGZ and, given its strict connection to the process of angiogenesis, is rather likely that also the process of angiogenesis is delimited in such region and, to some extent, in the granular layer. Since I analysed areas sampled within the hilar region of the DG it is understandable that my results do not show a particular high level of capillarization. But this may also be a starting point for new pathways in the study of brain capillarization, since it would be really interesting to verify if differences in the microvasculature arrangement exist not only between subregions of the hippocampus but also within the anatomical layers that constitute them.

## 5. Conclusions

A staining and quantification methods for the visualization of capillaries in brain tissue of diving mammals were here assessed. The anti-collagen IV staining technique was revealed to be very easy to perform and effective in both marine and terrestrial mammals. The “automatized method” for the quantification of the surface occupied by capillaries resulted to be more efficient and reliable than the “counting crosses method”, mostly because of the higher quality and clarity of the images obtained but also because is less time consuming. It is concluded that the anti-collagen-IV staining combined to the “automatized method” can be used for a correct quantitative analysis of the capillarization of the cerebral tissue, in both diving and non-diving species.

My findings confirmed that differences in capillarization exist not only between species, but also between and within brain regions. Particularly, the grey matter was shown to have a denser capillarization than the white matter both in cerebral and cerebellar cortex, independently of the species. As well as the white matter, the medulla was found to have a very low level of capillarization compared to the other cerebral regions. Also, within the hippocampus, the CA1 showed a capillary density consistently greater than the other two hippocampal subregions analysed, the CA3 and the dentate gyrus. Such differences are directly correlated to the different metabolic demands of each region that were found in previous studies. In all the brain regions analysed, a higher capillarization was reported for the diving species compared to the non-diving one, confirming my hypothesis that an improved brain capillarization can be present in diving mammals as an adaptation to their repeated exposure to hypoxia. However, because of limited access to samples, further investigations are needed to better assess and verify such hypothesis.

## 6. References

- Aitken P.G. and Schiff S.J. (1986) Selective neuronal vulnerability to hypoxia in vitro. *Neuroscience Letters* 67: 92-96
- Alroy J., Goyal V. and Skutelsky E., (1987) Lectin histochemistry of mammalian endothelium. *Histochemistry* 86: 603 – 607
- Alturkistani H.A., Tashkandi F.M. and Mohammedsaleh Z.M. (2016) Histological stains: a literature review and case study. *Global Journal of Health Science* Vol.8, No. 3, 72-79
- Amaral D.G., Scharfman H.E. and Lavenex P. (2007) The dentate gyrus: fundamental neuroanatomical organization (dentate gyrus for dummies) *Progress in Brain Research* 163: 3-22
- Andersen H.T. (1975) Capillary density in skeletal muscle of man. *Acta physiol. scand.* 95 :203-205
- Andersen J.M., Skern-Mauritzen M., Boehme L., Wiersma Y.F., Rosing-Asvid A., Hamill M.O., Stenson G.B. (2013) Investigating Annual Diving Behaviour by Hooded Seals (*Cystophora cristata*) within the Northwest Atlantic Ocean. *PLoS ONE* 8(11): e80438.
- Andersen P. and Henriksson J. (1977) Capillary supply of the quadriceps femoris muscle of man: adaptive response to exercise. *J. Physiol.* 270: 677-690
- Attwell D and Laughlin S.B. (2001) An energy budget for signaling in the grey matter of the brain. *Journal of Cerebral Blood Flow and Metabolism* 21: 1133-1145
- Bannister R.G. and Romanul F.C.A. (1963) The localization of alkaline phosphatase activity in cerebral blood vessels. *J. Neurol. Neurosurg. Psychiat.* 26: 333-340
- Beach T.G., Tago H., Nagai T., Kimura H., McGeer O.L. and McGeer E.G. (1987) Perfusion-fixation of the human brain for immunohistochemistry: comparison with immersion-fixation. *Journal of Neuroscience Medicine* 19:183-192
- Bell M.A. and Ball M.J. (1985) Laminar variation in the microvascular architecture of normal human visual cortex (area 17). *Brain Research* 335: 139-143
- Bell M.A. and Ball M.J. (1981) Morphometric comparison of hippocampal microvasculature in ageing and demented people: dimeters and densities. *Acta Neuropathol. (Berl.)* 53: 299-318
- Bennett H.S., Luft J.H. and Hampton J.C. (1959) Morphological classification of vertebrate blood capillaries. *Am. J. Physiol.* 196 (2): 381-390
- Bittar P.G., Charnay Y., Pellerin L., Bouras C. And Magistretti P.J. (1996) Selective distribution of lactate dehydrogenase isoenzymes in neurons and astrocytes of human brain. *Journal of Cerebral Blood Flow and Metabolism* 16: 1079-1089
- Blix A. S. and From S. H. J. (1971) Lactate dehydrogenase in diving animals – a comparative study with special reference to the eider (*Somateria mollissima*) *Comp. Biochem. Physiol.* Vol. 40B: 579-584
- Blix A. S., Elsnér R., Kjenkshus J. K. (1983): Cardiac output and its distribution through capillaries and A-V shunts in diving seals. *Acta Physiol. Scand.*, 118: 109-116
- Blix A.S. (1987) Diving responses: fact or fiction. *Physiology*, 2 (2), 64-66
- Blix A.S. (2005) Arctic animals. Tapir Academic press, Trondheim.
- Boero J.A., Ascher J., Arregui A., Rovainen C. and Woosley T.A. (1999) Increased brain capillaries in chronic hypoxia. *J. Appl. Physiol.* 86 (4): 1211-1219
- Boutilier R.G. (2001) Mechanisms of cell survival in hypoxia and hypothermia. *The Journal of Experimental Biology* 204: 3171-3181
- Bowen W.D., Oftedal O.T., Boness D.J. (1985) Birth to weaning in 4 days: remarkable growth in the hooded seal, *Cystophora cristata*. *Can J. Zool.* 63:2841-2846

- Burns J.M., Lestyk K.C., Folkow L.P., Hammill M.O., Blix A.S. (2007) Size and distribution of oxygen stores in harp and hooded seals from birth to maturity. *J Comp Physiol. B* 177: 687-700
- Butler P.J. and Jones D.R. (1997) Physiology of diving of birds and mammals. *Physiol. Rev* 77:837-899
- Cahn R.D., Kaplan N.O., Levine L. and Zwilling E. (1962) Nature and development of lactic dehydrogenases. *Science*, New Series, Vol. 136, No. 3520: 962-969
- Cajal S.R. (1911) *Histologie du Systeme Nerveux de l'Homme et des Vertebretes*. Vol. 1 and 2, A. Maloine, Paris.
- Cao L., Jiao X., Zuzga D.S., Liu Y., Fong D.M., Young D. and During M. (2004) VEGF links hippocampal activity with neurogenesis, learning and memory. *Nature Genetics* 36 (8): 827-835
- Cardoso F.L., Brites D. and Brito M.A. (2010) Looking at the blood-brain barrier: molecular anatomy and possible investigation approaches. *Brain Research Reviews* 64: 328-363
- Cavaglia M., Dombrowski S.M., Drazba J., Vasanji A., Bokesch P.M. and Janigro D. (2001) Regional variation in brain capillary density and vascular response to ischemia. *Brain Research* 910: 81-93
- Čebašek V., Kubínová L., Ribarič S., Eržen I. (2004) A novel staining method for quantification and 3D visualization of capillaries and muscle fibers. *European Journal of Histochemistry* Vol. 48, Issue 2: 151-158
- Celik I., Seker M. and Salbacak A. (2018) Histological and histomorphometric studies of the cerebellar cortex and silver stained nucleolus organizer of Purkinje neurons in chronic morphine-treated rats. *Veterinarki Arhiv* 88 (1): 75-88
- Cocks M., Shaw C.S., Shepherd S.O., Fisher J.P., Ranasinghe A.M., Barker T.A., Tipton K.D., Wagenmakers A.J. (2013) Sprint interval and endurance training are equally effective in increasing muscle microvascular density and eNOS content in sedentary males. *J Physiol* 591.3: 641-656
- Crone C. (1963) The permeability of capillaries in various organs as determined by use of the "indicator diffusion" method. *Acta physiol. scand.* 58: 292-305
- Czéh B., Abumaria N., Rygula R. and Fuchs E. (2010) Quantitative changes in hippocampal microvasculature of chronically stressed rats: no effect of fluoxetine treatment. *Hippocampus* 20:174-185
- Damon D.H. and Duling B. (1984) Distribution of capillary blood flow in the microcirculation of the hamster: an *in vivo* study using epifluorescent microscopy. *Microvascular Research* 27, 81-95
- Davies H.G., Barter R. and Danielli J.F. (1954) A quantitative method for enzyme cytochemistry applied to alkaline phosphatase. *Nature* Vol. 173 No. 4417: 1234 – 1235
- Dawson D.M., Goodfriend T.L. and Kaplan N.O. (1964) Lactic dehydrogenases: functions of the two types. *Science*, New Series, Vol. 143, No. 3609: 929-933
- Delesse M.A. (1847) Procédé mécanique pour déterminer la composition des roches. *C R Acad Sci Paris* 25: 544-545
- Dirangl U., Iadecola C. and Moskowitz M.A. (1999) Pathobiology of ischaemic stroke: an integrated view. *Trends Neurosci.* 22: 391-397
- Dormer K.J., Denn M.J., Stone. H.L. (1977): Cerebral blood flow in the sea lion (*Zalophus Californianus*) during voluntary dives. *Comp. Biochem. Physiol.*, A 58: 11-18
- Elsner R., Shurley J. T., Hammond D. D. and Brooks R.E. (1970) Cerebral tolerance to hypoxemia in asphyxiated Weddell seals. *Respiration Physiology* 9: 287-297
- Erecinska M. and Silver I.A. (1989) ATP and brain function. *Journal of cerebral blood flow and metabolism* 9:2-19

- Erecinska M. and Silver I.A. (1994) Ions and energy in mammalian brain. *Progress in Neurobiology* 43: 37-71
- Erecinska M. and Silver I.A. (2001): Tissue oxygen tension and brain sensitivity to hypoxia. *Respiration physiology*, 128: 263-276
- Eriksson P.S., Perfilieva E., Björk-Eriksson T., Alborn A.M., Nordborg C., Peterson D.A. and Gage F.H. (1998) Neurogenesis in the adult human hippocampus. *Nature Medicine* Vol. 4 (11): 1313-1317
- Folkow L.P., Blix A.S. (1999) Diving behaviour of hooded seals (*Cystophora cristata*) in the Greenland and Norwegian Seas. *Polar Biol.* 22:61-74
- Folkow L.P., Mårtensson P.E., Blix A.S. (1996) Annual distribution of hooded seals (*Cystophora cristata*) in the Greenland and Norwegian Seas. *Polar Biol.* 16: 179-189
- Folkow L.P., Nordøy E.S., Blix A.S. (2004) Distribution and diving behaviour of harp seals (*Pagophilus groenlandicus*) from the Greenland Sea stock. *Polar Biol.* 27:281-298
- Folkow L.P., Ramirez J.M., Ludvigsen S., Ramirez N., Blix A.S. (2008): Remarkable neuronal hypoxia tolerance in the deep-diving adult hooded seal (*Cystophora cristata*). *Neuroscience Letters* 446: 147-150
- Forsythe J.A., Jiang B.H., Iyver N.V., Agani F., Leung S.W., Koos R.D., Semenza G.L. (1996) Activation of vascular endothelial growth factor gene transcription by hypoxia-inducible factor 1. *Molecular and Cellular Biology* Vol. 16, No. 9: 4604-4613
- Francois-Dainville E., Buchweitz E. and Weiss H.R. (1986) Effect of hypoxia on percent of arteriolar and capillary beds perfused in the rat brain. *J. Appl. Physiol.* 60(1): 280-288
- Friede R.L. (1965) A quantitative mapping of alkaline phosphatase in the brain of the rhesus monkey. *Journal of Neurochemistry* Vol.13 :197-203
- Geiseler S.J., Larson J., Folkow L.P. (2016): Synaptic transmission despite severe hypoxia in hippocampal slices of the deep-diving hooded seal. *Neuroscience* 334: 39-46
- Geyer G., Linss W., Makovitzky J. (1978) Electron microscopic toluidine blue staining of erythrocyte membrane. *Anat. Anz.* 143:291-4.
- Ghazarian H., Idoni B. and Oppenheimer S.B. (2011) A glycobiology review: carbohydrates, lectins, and implications in cancer therapeutics. *Acta Histochem.* 113 (3): 236-247
- Glezer I.I., Jacobs M.S., Morgane P.J. (1987) Ultrastructure of the blood-brain barrier in the dolphin (*Stenella coeruleoalba*) *Brain Research* 414: 205-218
- Gomori G. (1941) The distribution of phosphatase in normal organs and tissues, *J. Cell. and Cutup. Physiol.* 17: 71.
- Gomori, G. (1939) Microtechnical demonstration of phosphatase in tissue sections. *Proc. Soc. Exp. Biol. and Ailed.* 42: 23.
- Granger H.J. and Shepherd A.P., Jr. (1973) Intrinsic microvascular control of tissue oxygen delivery. *Microvascular research* 5: 49-72
- Gregersen M.I. and Rawson R.A. (1959) Blood volume. *Physiological Reviews* 39(2): 307-342
- Gunn A. (2016) *Rangifer tarandus*. *The IUCN Red List of Threatened Species 2016*: e.T29742A22167140.<http://dx.doi.org/10.2305/IUCN.UK.20161.RLTS.T29742A22167140.en>
- Hansen-Smith F., Banker K., Morris L. and Joswiak G. (1992) Alternative histochemical markers for skeletal muscle capillaries: a statistical comparison among three muscles. *Microvascular Research* 44, 112-116
- Harris J.J. and Attwell D. (2012) The energetics of CNS white matter. *The Journal of Neuroscience* 32(1): 356-371
- Hather B.M., Tesch P.A., Buchanan P., Dudley G.A. (1991) Influence of eccentric actions on skeletal muscle adaptations to resistance training. *Acta Physiol. Scand.* 143: 177-185
- Hill R.D., Schneider R.C., Liggins C.G., Schuette A.H., Elliott R.L., Guppy M., Hochachka P.W., Qvist J., Falke K.J. and Zapol W.M. (1987) Heart rate and body temperature

- during free diving of Weddell seals. *Am. J. Physiol.* 253 (Regulatory Integrative Comp. Physiol. 22): R344-R351
- Hill R.W., Wyse G.A. and Anderson M. (2012) *Animal physiology*. Third Edition, Sinauer Associates, Incl. Publishers. Sunderland, Massachusetts
- Hoff M.L.M., Fabrizius A., Folkow L.P. and Burmester T. (2016) An atypical distribution of lactate dehydrogenase isoenzymes in the hooded seal (*Cystophora cristata*) brain may reflect a biochemical adaptation to diving. *J. Comp. Physiol. B.* 186: 373-386
- Howart C., Peppiatt-Wildman C.M. and Attwell D. (2010) The energy use associated with neural computation in the cerebellum. *Journal of Cerebral Blood Flow & Metabolism* 30: 403-414
- Howarth C., Gleeson P. and Attwell D. (2012) Updated energy budgets for neural computation in the neocortex and cerebellum. *Journal of Cerebral Blood Flow & Metabolism* 32: 1222-1232
- Hunziker O., Frey H. and Schulz U. (1974) Morphometric investigations of capillaries in the brain cortex of the cat. *Brain Research* 65: 1-11
- Imdahl A. and Hossman K. A. (1986) Morphometric evaluation of post-ischemic capillary perfusion in selectively vulnerable areas of gerbil brain. *Acta Neuropathol.* 69: 267-271
- Jensen L., Bangsbo J., Hellsten Y. (2004) Effect of high intensity training on capillarization and presence of angiogenic factors in human skeletal muscle. *J Physiol* 557.2: 571-582
- Jesmin S., Hattori Y., Sakuma I., Liu M.Y., Mowa C.N. and Kitabatake A. (2003) Estrogen deprivation and replacement modulate cerebral capillary density with vascular expression of angiogenic molecules in middle-aged female rats. *Journal of Cerebral Blood Flow & Metabolism* 23: 181-189
- Kadar T., Dachir S., Shukitt-Hale B. and Levy A. (1998) Sub-regional hippocampal vulnerability in various animal models leading to cognitive dysfunction. *J Neural Transm* 105: 987-1004
- Kaplan M.S. and Hinds J.W. (1977) Neurogenesis in the adult rat: electron microscopic analysis of light radioautographs. *Science*, New Series, Vol. 197, Issue 4308, 1092-1094
- Karnovsky M.J. (1961) Simple methods for "staining with lead" at high pH in electron microscopy. *J. Biophys. Biochem. Cytol.* 11: 729-732
- Kerem D. and Elsner R. (1973): Cerebral tolerance to asphyxia hypoxia in the harbor seal. *Respiration Physiology* 19: 188-200
- Klein B., Kuschinsky W., Schrock H. and Vetterlein F. (1986) Interdependency of local capillary density, blood flow, and metabolism in rat brains. *Am. J. Physiol.* 251 (Heart Circ. Physiol. 20): H1333-H1340
- Kolinko Y., Cendelin J., Kralickova M. and Tonar Zbynek (2016) Smaller absolute quantities but greater relative densities of microvessels are associated with cerebellar degeneration in lurcher mice. *Front. Neuroanat.* 10-35
- Kovacs K.M. (2015) *Pagophilus groenlandicus*. *The IUCN Red List of Threatened Species 2015*:e.T41671A45231087.<http://dx.doi.org/10.2305/IUCN.UK.20154.RLTS.T41671A45231087.en>
- Kovacs K.M. and Lavigne D.M. (1985). Neonatal growth and organ allometry of Northwest Atlantic harp seals (*Phoca groenlandica*). *Can. J. Zool.* 63: 2793 - 2799.
- Kovacs K.M. and Lavigne D.M. (1986) *Cystophora cristata*. *Mammalian species* 258: 1-9
- Krogh A. (1918) The number and distribution of capillaries in muscles with calculations of the oxygen pressure head necessary for supplying the tissue. *J. Physiol.* 52: 409-415
- Krogh A. (1922). *The anatomy and physiology of capillaries* (Vol. 18). Yale University Press
- Kubíková T., Kochova P., Tomášek P., Witter K., Tonar Z. (2018) Numerical and length densities of microvessels in the human brain: correlation with preferential orientation of

- microvessels in the cerebral cortex, subcortical grey matter and white matter, pons and cerebellum. *Journal of Chemical Neuroanatomy* 88: 22-32
- Kuhn H.G., Dickinson-Anson H. and Gage F.H. (1996) Neurogenesis in the dentate gyrus of the adult rat: age-related decrease of neuronal progenitor proliferation. *The Journal of Neuroscience* 16(6): 2027-2033
- Kuzu I., Bicknell R., Harris A.L., Jones M., Gatter K.C. and Mason D.Y. (1992) Heterogeneity of vascular endothelial cells with relevance to diagnosis of vascular tumours. *J. Clin. Pathol.* 45: 143-148
- LaManna J.C., Chavez J.C., Pichiule P. (2004) Structural and functional adaptation to hypoxia in the rat brain. *The Journal of Experimental Biology* 207: 3163-3169
- LaManna J.C., Venel L.M., Farrell R.M. (1992) Brain adaptation to chronic hypobaric hypoxia in rats. *J. Appl. Physiol.* 72(6): 2238-2243
- Larson J., Drew K.L., Folkow L.P., Milton S.L., Park T.J. (2014): No oxygen? No problem! Intrinsic brain tolerance to hypoxia in vertebrates. *The Journal of Experimental Biology* 217: 1024-1039
- Laurie G.W., Leblond C.P. and Martin G.R. (1982) Localization of type IV collagen, laminin, heparan sulphate proteoglycan, and fibronectin to the basal lamina of basement membranes. *The Journal of Cell Biology* Vol. 95: 340-344
- Laurie G.W., Leblond C.P., Cournil I. and Martin G.R. (1980) Immunohistochemical evidence for the intracellular formation of basement membrane collagen (type IV) in developing tissues. *The Journal of Histochemistry and Cytochemistry* Vol. 28 No. 12: 1267-1274
- Leblond J. and Krenjević K. (1989) Hypoxic changes in hippocampal neurons. *Journal of Neurophysiology.* Vol. 62: 1-14
- Lenfant C, Johansen K. and Torrance J.D. (1970) Gas transport and oxygen storage capacity in some pinnipeds and the sea otter. *Respiration Physiology* 9, 277-286
- León-Velarde F., Sanchez J., Bigard A.X., Brunet A., Lesty C., Monge-C C. (1993) High altitude adaptation in Andean coots: capillarity, fiber area, fiber type and enzymatic activities of skeletal muscle. *J Comp Physiol. B* 163: 52-58
- Lestyk K.C., Folkow L.P., Blix A.S., Hammill M.O., Burns J.M. (2009) Development of myoglobin concentration and acid buffering capacity in harp (*Pagophilus groenlandicus*) and Hooded (*Cystophora cristata*) seals from birth to maturity. *J Comp Physiol. B* 179:985-996  
*Letters* 67: 92-96
- Lipton P. (1999) Ischemic cell death in brain neurons. *Physiological Reviews* Vol. 70, No. 4: 1432-1532
- Løkkegaard A., Nyengaard J.R. and West M.J. (2001) Stereological estimates of number and length of capillaries in subdivisions of the human hippocampal region. *Hippocampus* 11: 726-740
- Ludvigsen S. (2010) Neuronal Hypoxia tolerance in diving endotherms. PhD diss., University of Tromsø – The Arctic University of Norway – UiT, <https://hdl.handle.net/10037/2788>
- Lutz P.L., Nilsson G.E., Prentice H.M. (2003) The brain without oxygen. Third Edition, Kluwer Academic Publishers
- Lydersen C., Kovacs K.M. (1993) Diving behaviour of lactating harp seal, *Phoca groenlandica*, females from the Gulf of St Lawrence, Canada. *Anim. Behav.* 46:1213-1221
- Madsen K. and Holmskov U. (1995) Capillary density measurements in skeletal muscle using immunohistochemical staining with anti-collagen type IV antibodies. *Eur. J. Appl. Physiol.* 71: 472-274
- Mahyew T.M. (1992) A review of recent advances in stereology for quantifying neural structure. *Journal of Neurocytology* 21, 313-328



- Mandarim-De-Lacerda C.A. (2003) Stereological tools in biomedical research. *Anais da Academia Brasileira de Ciências* 75(4): 469-486
- Markert C.L. (1963) Lactate dehydrogenase isozymes: dissociation and recombination of subunits. *Science*, New Series, Vol. 140 No. 3573: 1329-1330
- Mathieu-Costello O., Agey P.J., Wu L., Szewczak J.M., MacMillen R.E. (1998) Increased fiber capillarization in flight muscle of finch at altitude. *Respiration Physiology* 111: 189-199
- Meir J.U., Champagne C.D., Costa D.P., Williams C.L., Ponganis P.J. (2009) Extreme hypoxic tolerance and blood oxygen depletion in diving elephant seals. *Am. J. Physiol. Regul. Integr. Comp. Physiol.* 297: R927-R939
- Meryman H.T. (1971) Cryoprotective agents. *Cryobiology* Vol. 8, No. 2, 173-183
- Mitz S.A., Reuss S., Folkow L.P., Blix A.S., Ramirez J.M., Hankeln T. and Burmester T. (2009) When the brain goes diving: glial oxidative metabolism may confer hypoxia tolerance to the seal brain. *Neuroscience* 163: 552-560
- Morland C., Andersson K.A., Haugen Ø. P., Hadzic A., Kleppa L., Gille A., Rinholm J.E., Palibrk V., Diget E.H., Kennedy L.H., Stølen T., Hennestad E., Moldestad O., Cai Y., Puchades M., Offermanns S., Vervaeke K., Bjørås M., Wisløff U., Storm-Mathisen J. and Bergersen L.H. (2017) Exercise induces cerebral VEGF and angiogenesis via the lactate receptor HCAR1. *Nat. Commun.* 8, 15557
- Murdaugh H.V., Seabury J.C. and Mitchell W.L. (1961) Electrocardiogram of the diving seal. *Circulation Research* IX: 358-361
- Murphy B., Zapol W.M. and Hochachka P.W. (1980) Metabolic activities of heart, lung, and brain during diving and recovery in the Weddell seal. *J. Appl. Physiol.: Respirat. Environ. Exercise Physiol.* 48(4): 596-605
- Nemeth P.M. and Lowry O.H. (1984) Myoglobin levels in individual human skeletal muscle fibers of different types. *The Journal of Histochemistry and cytochemistry* Vol. 32 No.11: 1211-1216
- Nicholson C. (2001): Diffusion and related transport mechanisms in brain tissue. *Rep. Prog. Phys.* 64: 815-884
- Nordøy E.S., Folkow L.P., Potelov V., Prischemikhin V. and Blix A.S. (2008) Seasonal distribution and dive behaviour of harp seals (*Pagophilus groenlandicus*) of the White Sea-Barents Sea stock. *Polar Biol.* 31: 1119-1135
- O'Brien J. And Sampson E.L. (1965) Lipid composition of the normal human brain: grey matter, white matter, and myelin. *Journal of Lipid Research* 6, 537-544
- Ohab J.J., Fleming S., Blesch A. and Carmichael S.T (2006) A neurovascular niche for neurogenesis after stroke. *The Journal of Neuroscience* 26 (50): 13007-13016
- Otrock Z.K., Mahfouz R.A.R., Makarem J.A. and Shamseddine A.I. (2007) Understanding the biology of angiogenesis: review of the most important molecular mechanisms. *Blood Cells, Molecules, and Diseases* 39: 212-220
- Paddock S.W. (2000) Principles and practices of laser scanning confocal microscopy. *Molecular Biotechnology* Vol. 16, 127-149
- Palmer T.D, Willhoite A.R. and Gage F.H. (2000) Vascular niche for adult hippocampal neurogenesis. *The Journal of Comparative Neurology* 425: 479-494
- Patt S., Sampaolo S., Théallier-Jankó A., Tschairkin I., Cervós-Navarro J. (1997) Cerebral angiogenesis triggered by severe hypoxia displays regional differences. *J. Cereb. Blood Flow Metab.* 17: 801-806
- Persidsky Y., Ramirez S.H., Haorah J., Kanmogne G.D. (2006) Blood-brain barrier: structural components and function under physiologic and pathologic conditions. *J Neuroimmun. Pharmacol.* 1: 223-236

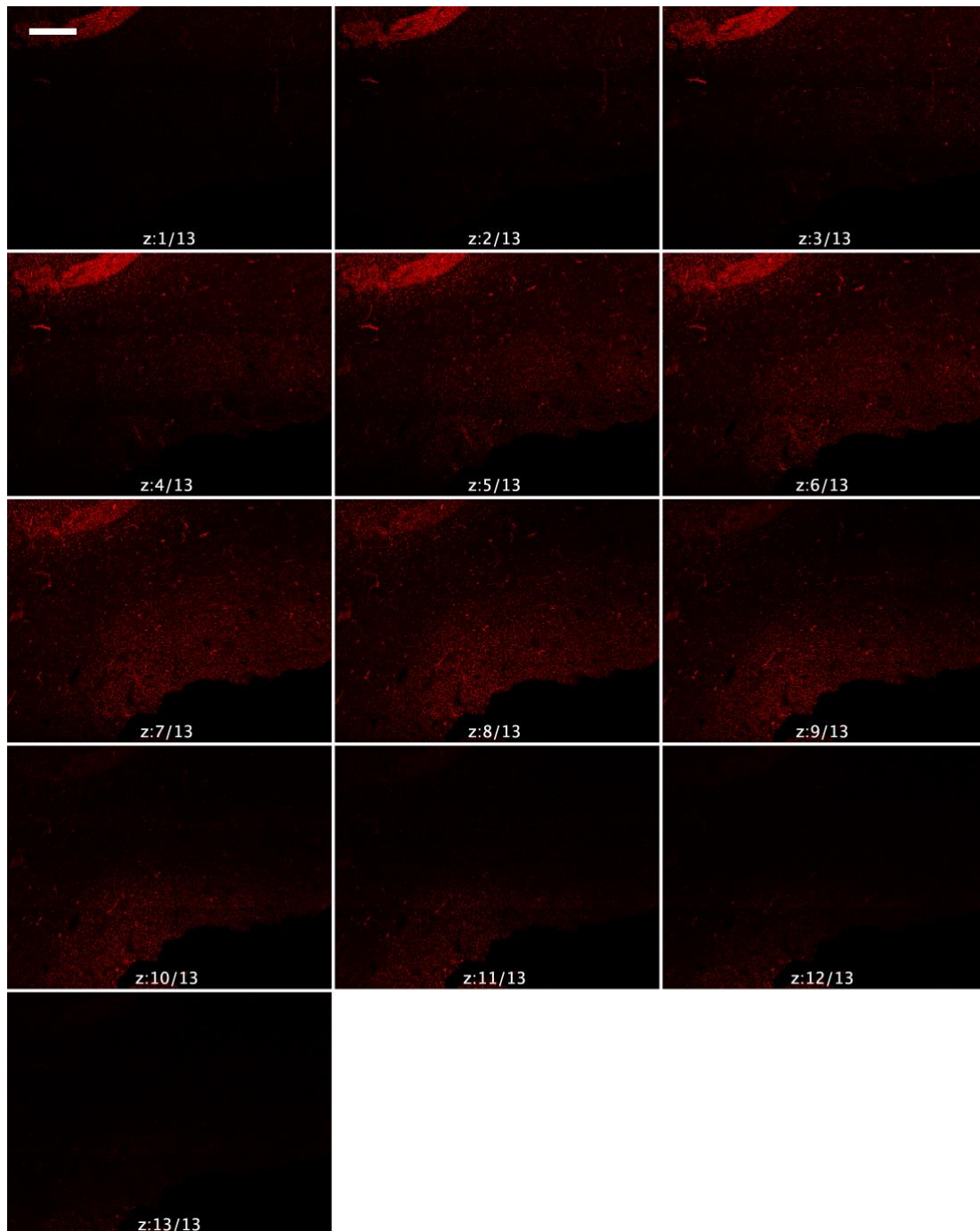
- Pusztaszeri M.P., Seelentag W. and Bosman F.T. (2006) Immunohistochemical expression of endothelial markers CD31, CD34, von Willebrand Factor, and Fli-1 in Normal Human Tissues. *Journal of Histochemistry and Cytochemistry* Vol. 54 (4): 385 -395
- Qu Z., Andersen J.L. and Zhou S. (1997) Visualization of capillaries in human skeletal muscle. *Histochem Cell Biol* 107: 169-174
- Qvist J., Hill R.D., Schneider R.C., Falke K.J., Liggins G.C., Guppy M., Elliot R.L., Hochachka P.W., Zapol W.M. (1986): Hemoglobin concentrations and blood gas tensions of free-diving Weddell seals. *J. Appl. Physiol.* 61: 1560-1569.
- Ramirez J.M., Folkow L.P., Blix A.S. (2007): Hypoxia tolerance in mammals and birds: from the wilderness to the clinic. *Annu. Rev. Physiol.* 69: 113-143.
- Romanul F.C.A. and Bannister R.G. (1962) Localized areas of high alkaline phosphatase activity in the terminal arterial tree. *The Journal of Cell Biology* 15: 73-84
- Rosene D.L., Roy N.J. and Davis B.J. (1986) A cryoprotection method that facilitates cutting frozen sections of whole monkey brains for histological and histochemical processing without freezing artifacts. *The Journal of Histochemistry and Cytochemistry* Vol.34, No. 10, pp. 1301-1315
- Rufaihah A.J., Huang N.F., Jamé S., Lee J.C., Nguyen H.N., Byers B., De A. Okogbaa J., Rollins M., Reijo-Pera R., Gambhir S.S. and Cooke J.P. (2011) Endothelial cells derived from human iPSCs increase capillary density and improve perfusion in a mouse model of peripheral arterial disease. *Arterioscler. Thromb. Vasc. Biol.* 31:e72-e79
- Russell T.H., Agey P.J., Hazel- wood L., Szewczak J.M., MacMillen R.E., and Mathieu-Costello O. (1998) Increased capillarity in leg muscle of finches living at altitude. *J. Appl. Physiol.* 85(5): 1871– 1876
- Saltin B. (1985) Hemodynamic adaptations to exercise. *Am. J. Cardiol.* 55: 42D-47D
- Scharfman H.E. and Myers C.E. (2013) Hilar mossy cells of the dentate gyrus: a historical perspective. *Frontiers in Neural Circuits* 6, Vol. 6, Article 106
- Schmidt-Kastner R. (2015) Genomic approach to selective vulnerability of the hippocampus in brain ischemia-hypoxia. *Neuroscience* 309, 259-279
- Schmidt-Kastner R. and Freund T.F. (1991) Selective vulnerability of the hippocampus in brain ischemia. *Neuroscience* Vol.40 No.3: 599-636
- Schmidt-Nielsen K. and Pennycuik P. (1961) Capillary density in mammals in relation to body size and oxygen consumption. *Am. J. Physiol.* 200 (4): 746-750
- Scholander P.F. (1940) Experimental investigations on the respiratory function in diving mammals and birds. No. 22. I kommisjon hos Jacob Dybwad.
- Seki T., Naito I., Oohashi T., Sado Y. And Ninomiya Y. (1998) Differential expression of type IV collagen isoforms  $\alpha 5(IV)$  and  $\alpha 6(IV)$  chains, in basement membranes surrounding smooth muscle cells. *Histochem. Cell Biol.* 110: 359-366
- Sergeant, D. E. (1991). Harp seals, man and ice. *Canadian special publication of fisheries and aquatic sciences/Publication speciale canadienne des sciences halieutiques et aquatiques.*
- Sergeant D.E. (1973) Transatlantic migration of harp seal, *Pagophilus groenlandicus*. *J. Fish. Res. Board Can.* 30: 124-125
- Shi S.R., Cote R.J. and Taylor C.R. (2001) Antigen retrieval techniques: current perspectives. *The Journal of Histochemistry & Cytochemistry* Vol. 49, No. 8, 931-937
- Stephens H.R., Duance V.C., Dunn M.J., Bailey A.J. and Dubowitz V. (1982) Collagen types in neuromuscular diseases. *Journal of the Neurological Sciences* 53: 45-62
- Stephenson T.J., Griffiths D.W.R., and Mills P.M. (1986) Comparison of *Ulex europaeus* I lectin binding and factor VIII-related antigen as markers of vascular endothelium in follicular carcinoma of the thyroid. *Histopathology* 10:251–260

- Takamatsu H. (1939) Histologische und biochemische Studien fiber die Phosphatase. I. Histochemi- sche Untersuchungsmethodik der Phos- phatase und deren Verteilung in verschie- denen Organen und Geweben, *Trans. Soc. Path. Japon.* 29: 492.
- Teng H., Zhang Z.G., Wang L., Zhang R.L., Zhang L., Morris D., Gregg S.R., Wu Z., Jiang A., Lu M., Zlokovic B.V. and Chopp M. (2008) Coupling of angiogenesis and neurogenesis in cultured endothelial cells and neural progenitor cells after stroke. *Journal of Cerebral Blood Flow & Metabolism* 28, 764-771
- Thompson D. and Fedak M. A. (1993) Cardiac responses of grey seals during diving at sea. *J. exp. Biol.* 174: 139-164
- Tonar Z. (2017) Data for: Numerical and length densities of microvessels in the human brain: Basic mapping of differences between the cerebral cortex, subcortical grey matter and white matter, pons and cerebellum, Mendeley Data, v2<http://dx.org/10.17632/5jn9rdy74w.2#file-10d98410-22e3-49ae-80438bef6e18c818>
- Veloso A., Fernández R., Astigarraga E., Barreda-Gómez G., Manuel I., Giralt M.T., Ferrer I., Ochoa B., Rodríguez-Puertas R., Fernández J.A. (2011) Distribution of lipids in human brain. *Anal Bioanal. Chem.* 401: 89-101
- Weber B., Keller A.L., Reichold J. and Logothetis N.K. (2008) The microvascular system of the striate and exrtastriate visual cortex of the macaque. *Cerebral Cortex* 18: 2318-2330
- Weiss H.R., Buchweitz E., Murtha T.J. and Auletta M. (1982) Quantitative regional determination of morphometric indices of the total and perfused capillary network in the rat brain. *Circ. Res.* 51: 494-503
- West M.J. (2012) Introduction to stereology. *Cold Spring. Harb. Protoc.*; doi:10.1101/pdb.top070623
- Xu K., LaManna J.C. (2006): Chronic hypoxia and the cerebral circulation. *J. Appl. Physiol.* 100: 725-730.
- Yamamoto K., de Waard V., Fearn C. and Loskutoff D.J. (1998) Tissue distribution and regulation of murine von Willebrand Factor gene expression in vivo. *Blood* Vol. 92, No. 8: 2791-2801
- Zapol W.M., Liggins G.C., Schneider R.C., Qvist J., Snider M.T., Creasy R.K., Hochachka P.W., (1979): Regional blood flow during simulated diving in the conscious Weddell seal. *J. Appl. Physiol.: Respirat. Environ. Exercise Physiol.* 47(5): 968-973
- Zeller K., Rahner-Welsch S. and Kuschinsky W. (1997) Distribution of Glut1 transporters in different brain structures compared to glucose utilization and capillary density of adult rat brains. *Journal of Cerebral Blood Flow and Metabolism* 17: 204-209
- Zhang R.L., Chopp M., Roberts C., Liu X., Wei M., Nejad-Davarani S.P., Wang X. and Zhang Z.G. (2014) Stroke increases neural stem cells and angiogenesis in the neurogenic niche of the adult mouse. *PLoS ONE* 9(12): e113972.
- Zhao C., Deng W. and Gage F.H. (2008) Mechanisms and functional implications of adult neurogenesis. *Cell* 132, 645-660

## 7. Appendixes

### Appendix I: Optical sections in series

**Figure 18.** The series of optical sections obtained for VC of the hooded seal (K6-18) is here illustrated. It is clear that the first (1,2,3) and the last (10,11,12,13) optical sections do not show a very strong staining, while sections like n° 4 and 5 show too much background and, therefore, couldn't be used for the quantitative analysis. For this particular image, the optical section n° 8 was used, because it was the one with the better quality of staining. Scale bar, 500  $\mu$ m.



## Appendix II: Fiji macros

### 1. Macros Step 1

```
run("Duplicate...", "duplicate");
run("Z Project...", "projection=[Max Intensity]");
setForegroundColor(255, 255, 255);
run("Duplicate...", "duplicate");
run("Blue")
```

### 2. Macros Step 2

```
run("Crop");
setBackgroundcolor(255, 0, 0);
run("Clear Outside", "stack");
run("Duplicate...", "duplicate channels=2");
run("Measure");
saveAs("Results", "/Users/chiaraciccone/Desktop/Results.csv");
run("Despeckle");
run("Despeckle");
run("Duplicate...", " ");
setAutoThreshold("Default");
//run("Threshold...");
setAutoThreshold("Huang");
setThreshold(20, 255);
setThreshold(20, 255);
//setThreshold(20, 255);
setOption("BlackBackground", false);
run("Convert to Mask");
run("Duplicate...", " ");
run("Analyze Particles...", "size=10-Infinity display clear include
add");
```

## Appendix III: Results Table

**Table 2.** Data obtained for each cerebral region sampled. The surface occupied by the capillaries is presented as a percentage of the total area. Results for the "counting crosses method" (P1) are reported as mean percentage between replicates ( $n=3$ )  $\pm$  standard deviation (SD). Results from the "automatized method" (P2) are reported as an absolute value and are always expressed as percentage.

<i>Cerebellum</i>				
Species	ID	Matter	P1 (mean $\pm$ SD; %)	P2 (%)
<b>Harp</b>	G15-18	Grey	9.8 $\pm$ 0.61	14.25
		White	9.5 $\pm$ 1.56	11.7
<b>Harp</b>	G8-18	Grey	6.93 $\pm$ 1.22	10.08
		White	NA	NA
<b>Hooded</b>	K6-18	Grey	3.83 $\pm$ 0.89	5.18
		White	5.73 $\pm$ 1.25	5.25
<b>Reindeer</b>	10-10	Grey	3.43 $\pm$ 0.58	5.91
		White	3.8 $\pm$ 0.39	7.81
<b>Reindeer</b>	9-10	Grey	5.23 $\pm$ 0.68	5.2
		White	2.12 $\pm$ 0.30	1.54
<i>Frontal cortex</i>				
Species	ID	Matter	P1 (mean $\pm$ SD; %)	P2 (%)
<b>Harp</b>	G15-18	Grey	7.93 $\pm$ 0.47	6.05
		White	NA	NA
<b>Harp</b>	G8-18	Grey	11.3 $\pm$ 1.13	9.05
		White	4.26 $\pm$ 1.27	4.23
<b>Hooded</b>	K6-18	Grey	7.32 $\pm$ 1.81	16.88
		White	3.53 $\pm$ 0.63	4.25
<b>Reindeer</b>	10-10	Grey	5.03 $\pm$ 0.34	6.71
		White	1.3 $\pm$ 0.29	2.46
<b>Reindeer</b>	9-10	Grey	3.33 $\pm$ 1.53	3.76
		White	1.53 $\pm$ 0.26	2.12
<i>Visual Cortex</i>				
Species	ID	Matter	P1 (mean $\pm$ SD; %)	P2 (%)
<b>Harp</b>	G15-18	Grey	8.66 $\pm$ 0.82	8.08
		White	4.53 $\pm$ 0.53	2.98
<b>Harp</b>	G8-18	Grey	8.37 $\pm$ 1.89	9.63
		White	NA	NA
<b>Hooded</b>	K6-18	Grey	10 $\pm$ 0.55	13.72
		White	3.4 $\pm$ 0.21	4.77
<b>Reindeer</b>	10-10	Grey	5.66 $\pm$ 0.56	6.51
		White	1.97 $\pm$ 0.65	2.02
<b>Reindeer</b>	9-10	Grey	4.3 $\pm$ 1.59	1.8
		White	2.4 $\pm$ 1.10	1.17
<i>Medulla</i>				
Species	ID	Matter	P1 (mean $\pm$ SD; %)	P2 (%)
<b>Harp</b>	G15-18	White	3.1 $\pm$ 0.8	5.88
<b>Hooded</b>	K6-18	White	1.5 $\pm$ 0.59	3.41
<b>Reindeer</b>	10-10	White	0.96 $\pm$ 0.23	1.84
<b>Reindeer</b>	9-10	White	0.66 $\pm$ 0.11	0.98
<i>Hippocampus</i>				
Species	ID	Subregion	P1 (mean $\pm$ SD; %)	P2 (%)
<b>Harp</b>	G15-18	DG	5.46 $\pm$ 1.1	10.64
		CA3	6.92 $\pm$ 0.98	10.25

		CA1	7.2 ± 0.61	13.57
<b>Harp</b>	G8-18	DG	5.3 ± 0.88	6.08
		CA3	5.26 ± 0.77	7.06
		CA1	4.8 ± 1.1	8.38
<b>Hooded</b>	K6-18	DG	5.93 ± 0.14	7.66
		CA3	7.16 ± 1.25	10.05
		CA1	9.27 ± 1.17	13.82
<b>Reindeer</b>	9-10	DG	3.16 ± 0.56	4.72
		CA3	3.23 ± 0.46	4.82
		CA1	4.13 ± 0.94	7.86

**Table 3.** Comparison between the 5 different cerebral regions: Cerebellum (CB), Frontal cortex (FC), Hippocampus (HC), Medulla (MED) and Visual cortex (VC). For CB, FC and VC both the grey and white matter were considered. In HC all the subregions (CA1, CA3 and DG) were also considered. The p-values were obtained with a t-test in R (R Core team, 2013). For the values obtained considering the results of the “counting crosses method” (p1), n = means between replicates sampled for each region; For the values obtained with the results of the “automatized method” (p2), n = absolute values obtained for each sample analysed.

Regions compared	n	p-value	
		p1	p2
<b>CB-FC</b>	18	0.7083	0.5357
<b>CB-MED</b>	13	0.0027	0.0263
<b>CB-VC</b>	18	0.9287	0.363
<b>FC-MED</b>	13	0.0154	0.1212
<b>HC-CB</b>	21	0.9597	0.4198
<b>HC-FC</b>	22	0.633	0.1652
<b>HC-MED</b>	16	0.0004	0.0039
<b>HC-VC</b>	21	0.8771	0.0821
<b>VC-FC</b>	18	0.779	0.801
<b>VC-MED</b>	13	0.0047	0.1717

# Appendix IV: Comparison between the results obtained with the different methods

